Cell-based cccDNA reporter assay combined with functional genomics identifies YBX1 as HBV cccDNA host factor and antiviral candidate target

Eloi Verrier, Gaëtan Ligat, Laura Heydmann, Katharina Doernbrack, Julija Miller, Anne Maglott-Roth, Frank Jühling, Houssein El Saghire, Margaux J Heuschkel, Naoto Fujiwara, et al.

OPEN ACCESS

Original research

Cell-based cccDNA reporter assay combined with functional genomics identifies YBX1 as HBV cccDNA host factor and antiviral candidate target

Eloi R Verrier,[1] Gaëtan Ligat ,[1] Laura Heydmann,[1] Katharina Doernbrack,[2] Julija Miller,[2] Anne Maglott-Roth,[3] Frank Jühling,[1] Houssein El Saghire,[1] Margaux J Heuschkel,[1] Naoto Fujiwara ,[4] Sen-Yung Hsieh,[5] Yujin Hoshida,[4] David E Root,[6] Emanuele Felli,[1,7] Patrick Pessaux,[1,7] Atish Mukherji,[1] Laurent Mailly,[1] Catherine Schuster ,[1] Laurent Brino,[3] Michael Nassal ,[2] Thomas F. Baumert [1,7]

► Additional supplemental material is published online only. To view, please visit the journal online (http://dx.doi.org/10.1136/gutjnl-2020-323665).

For numbered affiliations see end of article.

Correspondence to
Prof. Thomas F. Baumert and Dr Eloi R Verrier, Strasbourg, France; Thomas.Baumert@unistra.fr, e.verrier@unistra.fr and Professor Michael Nassal, Freiburg, Germany; michael.nassal@uniklinik-freiburg.de

ERV and GL are joint first authors.
MN and TFB are joint senior authors.

Received 19 November 2020
Accepted 24 November 2022

To cite: Verrier ER, Ligat G, Heydmann L, *et al*. *Gut* Epub ahead of print: [*please include* Day Month Year]. doi:10.1136/gutjnl-2020-323665

ABSTRACT

Objectives Chronic hepatitis B virus (HBV) infection is a leading cause of liver disease and hepatocellular carcinoma. A key feature of HBV replication is the synthesis of the covalently close circular (ccc)DNA, not targeted by current treatments and whose elimination would be crucial for viral cure. To date, little is known about cccDNA formation. One major challenge to address this urgent question is the absence of robust models for the study of cccDNA biology.

Design We established a cell-based HBV cccDNA reporter assay and performed a loss-of-function screen targeting 239 genes encoding the human DNA damage response machinery.

Results Overcoming the limitations of current models, the reporter assay enables to quantity cccDNA levels using a robust ELISA as a readout. A loss-of-function screen identified 27 candidate cccDNA host factors, including Y box binding protein 1 (YBX1), a DNA binding protein regulating transcription and translation. Validation studies in authentic infection models revealed a robust decrease in HBV cccDNA levels following silencing, providing proof-of-concept for the importance of YBX1 in the early steps of the HBV life cycle. In patients, *YBX1* expression robustly correlates with both HBV load and liver disease progression.

Conclusion Our cell-based reporter assay enables the discovery of HBV cccDNA host factors including YBX1 and is suitable for the characterisation of cccDNA-related host factors, antiviral targets and compounds.

WHAT IS ALREADY KNOWN ON THIS TOPIC

⇒ Antiviral therapeutic strategies can control hepatitis B virus (HBV) infection, but viral cure is rarely observed.
⇒ Current antiviral therapies do not eliminate covalently close circular (ccc)DNA, HBV's persistence reservoir.
⇒ Knowledge about cccDNA formation and its host-dependency factors is limited.
⇒ DNA repair factors are expected to play a central role in cccDNA formation.

WHAT THIS STUDY ADDS

⇒ A cell-based reporter assay allows simple and robust quantification of cccDNA by ELISA.
⇒ The assay enables discovery of HBV cccDNA host factors.
⇒ A loss-of-function screen identified YBX1 as a previously undiscovered cccDNA-related HBV host factor that directly interacts with HBV DNA.
⇒ Silencing of YBX1 expression impairs HBV infection.
⇒ Gene expression analyses in patients suggest an association between YBX1 and virus-induced liver disease and cancer.

HOW THIS STUDY MIGHT AFFECT RESEARCH, PRACTICE OR POLICY

⇒ The cell-based cccDNA reporter assay will enable to discover urgently needed targets for viral cure in patients.

INTRODUCTION

Chronic infection by hepatitis B virus (HBV) is a major cause of advanced liver disease and hepatocellular carcinoma (HCC), the second-leading cause of cancer death worldwide.[1] Despite the availability of an effective prophylactic vaccine, an estimated 250 million people worldwide are chronic virus carriers.[2] While nucleos(t)ide analogues (such as tenofovir or entecavir) have been proven to effectively control HBV infection by suppression of viral replication, treatment is lifelong and viral cure remains extremely rare. PEG-IFN-α-based therapies can result in viral cure in a small subset of patients; however, these therapies are limited by a low response rate and significant side effects.[3]

HBV belongs to the *Hepadnaviridae* family, small enveloped retrotranscribing DNA viruses.[4] In infectious virions the genome is present as a 3.2 kb relaxed circular (rc) DNA in which one strand is covalently linked to the viral polymerase.[5] Following entry into hepatocytes through heparan-sulfate proteoglycan and the liver-specific sodium-taurocholate cotransporting polypeptide (NTCP) as high affinity receptor,[6] the nucleocapsid transports

the rcDNA to the nuclear pore for release into the nucleus. There, rcDNA is converted into an episomal covalently close circular (ccc)DNA minichromosome that serves as a template for all viral transcripts including pregenomic (pg) RNA,[7] which is encapsidated and reverse transcribed into new rcDNA. The rcDNA-containing nucleocapsids can be enveloped and released as virions or be recycled to the nucleus to replenish the cccDNA pool.[8] Hence cccDNA formation is key to HBV persistence.[7] A few cccDNA copies per liver cell can reactivate full virus production on therapy withdrawal, or on loss of immunological control over the low-level replication likely going on even under therapy. Any true cure of chronic HBV infection will require elimination of cccDNA.[7]

To date, the molecular basis of rcDNA to cccDNA conversion is poorly understood, largely due to the historic lack of feasible *in vitro* infection systems in which virus production is strictly dependent on cccDNA. Conceptual clues on the mechanism governing cccDNA formation come from the structural differences between the two DNAs. Accordingly, conversion comprises multiple steps, such as the release of the polymerase, trimming/fill-in of the DNA-strands, and eventually ligation. Given HBV's minimal coding capacity, the underlying activities are likely to come from the host cell, in particular the DNA repair machinery, a network of ~250 factors evolved to fix any deviation from a perfect double-stranded structure.[7] Based on this premise several recent studies unravelled the involvement of DNA repair factors in cccDNA formation. Tyrosyl-DNA-phosphodiesterase 2 (TDP2) was shown to be capable of releasing the bound polymerase from HBV and duck HBV (DHBV) rcDNA.[9] A DNA polymerase-targeted siRNA screen identified DNA polymerase K (POLK), a gamma-family DNA polymerase, as a key contributor to the completion of the positive strand for the conversion of deproteinised (DP-) rcDNA into cccDNA.[10] Flap endonuclease 1 (FEN1) has been shown to bind and cleave the 5'-flap structure of HBV rcDNA *in vitro* to promote cccDNA formation,[11] possibly representing an alternative, nucleolytic pathway towards DP-rcDNA. Most recently, proliferating cell nuclear antigen (PCNA), replication factor C complex, DNA polymerase δ (POLD), FEN-1 plus DNA ligase 1 (LIG1) were found as the minimal host factor set for *in vitro* conversion of rcDNA-like molecules into cccDNA forms.[12] However, the redundancies in the DNA repair machinery and even more the complex environment of an intact cell, including intracellular trafficking and metabolic turnover of the viral components, imply that cccDNA formation *in vivo* involves numerous additional host factors. Their identification will be crucial for a comprehensive understanding of HBV persistence as well the definition of new antiviral targets as a basis for a cure for chronic HBV infection; given their fundamental role in cellular DNA replication and apparent lack of HBV specificity the five minimally required already identified host factors are unlikely to make such targets.

In spite of the development of recent cell culture infection systems for HBV, a major limitation for the investigation of cccDNA formation is the limited number of cccDNA copies in infected cells.[13] Moreover, cccDNA quantification by qPCR is still not finally standardised while Southern blotting, which allows for unambiguous distinction of cccDNA from all other viral DNA forms, is an intrinsically insensitive method.[13] Hence, aiming to characterise novel cccDNA-related host factors we established in this study a novel cccDNA reporter cell line based on the >20 fold higher cccDNA copy numbers produced by DHBV in human HepG2 hepatoma cells.[8] Applying to this cell line a loss-of-function screening strategy using an shRNA library targeting the DNA repair machinery and subsequent validation in HBV infection models we uncover YBX1 as a new cccDNA-related HBV host factor.

RESULTS

A robust cell-based reporter assay models cccDNA formation using a simple ELISA-based readout for cccDNA quantification

To address the limitations of detection of low abundance of cccDNA for functional genomics, we established a cell-based cccDNA reporter assay (figure 1A), which enables the non-invasive monitoring of cccDNA through a simple and robustly quantifiable ELISA for the cccDNA-dependent generation of a secreted, haemagglutinin (HA) tagged viral antigen in a stable HepG2 cell line, termed HA2/3. One key feature to achieve robust cccDNA levels in this model is the use of an envelope-deficient DHBV genome which can boost cccDNA copy numbers per cell to>100 in avian yet also in human hepatoma cells.[8] In a first approach, an expression cassette wherein pgRNA transcription is controlled by a tetracycline (Tet) Response-Element (TRE) promoter was integrated into HepG2.TA2-7 cells[14] which stably express a Tet-transactivator (tTA); the tTA binds to and activates the TRE promoter only in the absence of Tet or its analogue doxycyclin (Dox). Hence Dox withdrawal from the culture medium induces pgRNA transcription. Owing to its dual function as mRNA for core protein (HBcAg for HBV, DHBcAg for DHBV) and polymerase and as substrate for reverse transcription into rcDNA this is sufficient to initiate intracellular replication. If cccDNA is formed from the rcDNA, pgRNA transcription comes under control of the authentic viral core promoter which, different from the TRE promoter, produces an additional, 5' extended transcript, the precore RNA (see figure 1A–C); this enables synthesis of the N terminally extended precore protein, precursor of the processed, secretory e antigen (HBeAg for HBV, DHBeAg for DHBV). Hence specific detection of eAg would indicate prior cccDNA formation, as previously proposed.[15] It is well established that HBcAg and HBeAg share largely identical primary sequences but adopt different three-dimensional structures.[16 17] Their serological discrimination relies largely on inaccessibility of epitopes in the assembled capsid and the scarcity of free capsids in serum, owing to immune complex formation. As this does not hold in cell culture, the naked HBV capsids known to be released from the cells,[18] especially when damaged, can mock the presence of HBeAg. Via side-by-side expression of HBV core and precore protein we demonstrated that this is as well an issue with DHBV since DHBcAg accumulated to comparable amounts in the culture supernatant as the glycosylated and non-glycosylated forms of DHBeAg (figure 2A). Hence, DHBeAg could only serve as surrogate marker for cccDNA if strictly DHBeAg-specific antibodies were available which they are not.

We, therefore, sought to introduce a tag into the preC sequence such that it is exclusively expressed as part of the precore protein, does not interfere with secretion, and remains on DHBeAg on processing. Two constructs with a HA tag inserted shortly upstream of the core open reading frame (DpCHA1, DpCHA2) met these criteria, as shown by the secretion of glycosylated, anti-HA detectable proteins of the expected size (figure 2A). An important concern was the overlap on the pgRNA level of the preC coding region with the Dε RNA stem-loop that acts as encapsidation signal and

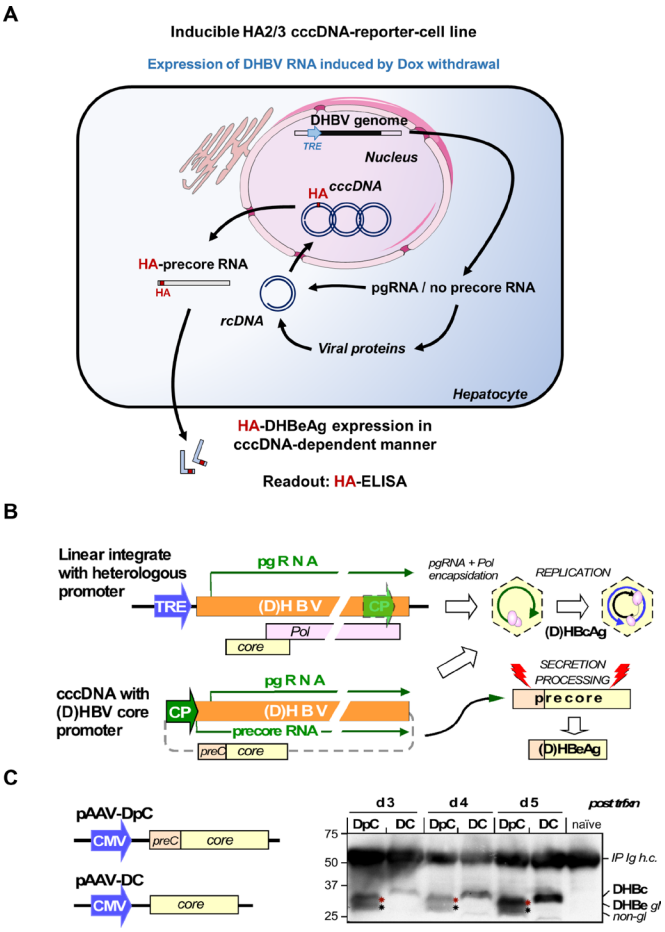

Figure 1 Use of secreted wild-type DHBeAg as non-invasive surrogate marker for cccDNA is frustrated by cellular release of DHBcAg. (A) Cartoon of the Tet-controlled HepG2 cell line expressing a modified full-length DHBV genome (with pgRNA expression under control of the Tet-responsive TRE promoter). Cells start producing DHBV RNA after removal of doxycycline (Dox) from the culture medium. expression of the DHBV envelope protein L is prevented by a premature stop codon. The cells synthesise no precore RNA whose start site would lie upstream of the start site defined by the TRE promoter. After pgRNA reverse transcription into DNA, DHBV DNA is recycled in the nucleus leading to the formation of cccDNA, which will serve as an additional template for viral transcription generating precore RNA and DHBV HBeAg (DHBeAg). Consequently, in this model, DHBeAg is a direct marker for cccDNA activity. In addition, a HA-tag encoding sequence was inserted into the precore region, before the start of the core ORF, leading to the production of a HA-tagged DHBeAg. (B) Assay principle. as mRNA for core protein and polymerase, and as substrate for reverse transcription pgRNA is sufficient to initiate hepadnaviral replication. Transcription of pgRNA from the authentic core promoter (CP) on cccDNA can be substituted by a heterologous promoter (eg, a Tet responsive TRE promoter) in front of a linear (D) HBV genome integrated into a plasmid or host chromosome. In this way no precore RNA and hence neither precore protein nor its prcessing product (D) HBeAg are generated (top). On circular cccDNA, the CP promoter controls pgRNA plus precore RNA transcription, supporting replication and (D) HBeAg synthesis (bottom). (C) Release of DHBcAg from cells obscures specific detection of DHBeAg. To mimic the translation products of pgRNA and precore RNA the ORFs for DHBV core (DC) and precore (DpC) proteins were expressed in transfected HepG2 cells from CMV promoter controlled pAAV vectors (left). Products in the culture supernatants were enriched by immunoprecipitation with a polyclonal anti-DHBc/e antiserum on days 3, 4 and 5 post-transfection and analysed by Western blotting. The DPC vectors produced a double band at about 27 and 30 kDa, as expected for non-glycosylated (non-gl, black stars) and glycosylated (gl, red stars) DHBeAg from DHBV16; clearly, however, also the DC vectors generated a specific band at about 30 kDa, as expected for DHBV core protein. Hence as reported for HBV,[19] also the core protein from DHBV can be released from cells, likely as non-enveloped capsids. Hence in the absence of a truly preC specific antibody the presence of DHBcAg prevents unambiguous detection of DHBeAg in an ELISA format, ablating the cccDNA dependency of the assay. Specificity can be regained by selective tagging of DHBeAg (see figure 2). cccDNA, covalently close circular DNA; CMV, cytomegalovirus; DHBV, duck hepatitis B virus; IP Ig h.c., heavy chain of the immunoglobulin used for immunoprecipitation.

replication origin for first-strand DNA synthesis; however, both constructs supported formation of wild-type like rc- and double-strand linear DNA (figure 2B) when part of the full DHBV genome in expression vector pCD16_env⁻. We therefore transfected an analogous TRE-promoter controlled DpCHA2 construct into HepG2.TA2-7 cells and, after evaluating various cell clones for cccDNA formation and HAeAg secretion, chose clone HA2/3 for all further experiments. Clonality of the cell line as well as efficient Dox regulation are supported by nearly all cells showing intracellular DHBcAg staining in the absence and very few cells staining positive in the presence of Dox. As shown in figure 2C, the accumulation of nuclear cccDNA around day 10 postinduction by Dox withdrawal was clearly reflected by a steep increase in HA signal intensity in the culture supernatant (monitored by a sandwich ELISA using a chromogenic substrate), attesting to secretion of HA-tagged DHBeAg as a valid surrogate marker for cccDNA formation. Furthermore,

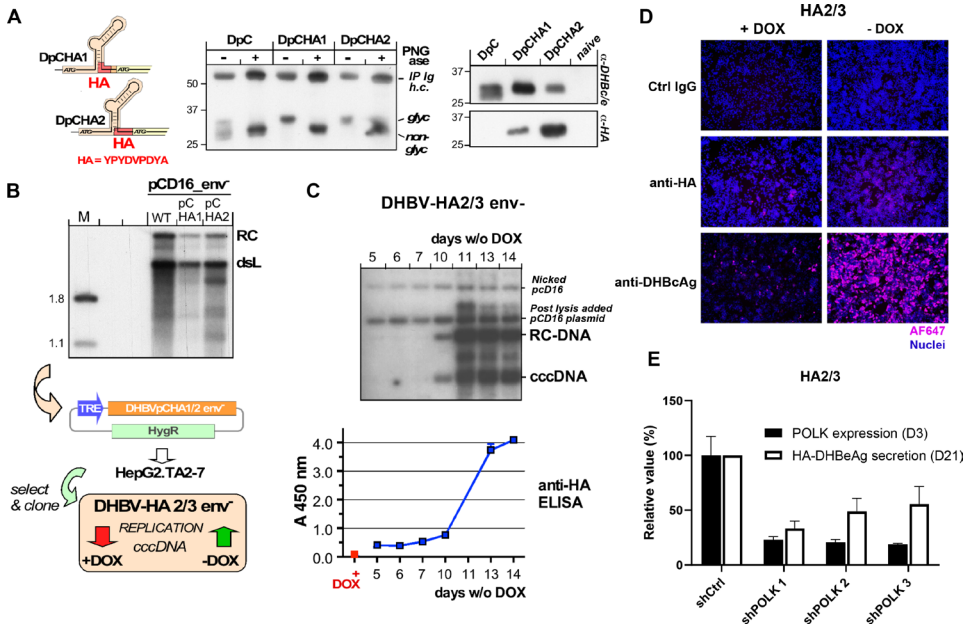

Figure 2 Strategically positioned HA-tags compatible with DHBV precore processing and replication. (A) glycosylation and retention of the HA-tag indicate DHBe-like secretion. constructs DpCHA1 and DpCHA2 differ in the insertion position of the HA-tag coding sequence in preC which is four amino acids upstream of the core ORF in DpCHA1, and immediately in front of the core ORF in DpCHA2 (left); the predicted signal sequence cleavage site (SignalP V3) is eight residues upstream. Vector pAAV-DpC and the HA-tag derivatives were transfected into HepG2 cells, and DHBc/e-reactive products in the culture supernatants were enriched by immunoprecipitiation. About one half of the immunopellet was treated with PNGase, the other half was not, then both were analysed by immunoblotting with polyclonal anti-DHBc/e antiserum (middle). While the doublet character of the main products from both HA-tag constructs was less pronounced than for the DPC construct, PNGase caused a similar mobility increase, indicating loss of glycosylation. Only the products from the HA-constructs were detected by a monoclonal anti-HA antibody (right), confirming that the secreted products contained the HA tag. (B) Replication competence. HepG2 cells were transfected with vector pCD16_env- encoding an envelope-deficient variant of wild-type DHBV16 (WT) and the respective pCHA1 and pCHA2 derivatives. Five days post-transfection viral DNAs from cytoplasmic capsids were analysed by southern blotting using a 32P-labelled DHBV DNA probe. although signals appeared slightly weaker than those from WT, both PchA derivatives clearly supported dsL and rc-DNA formation. The pCHA-modified DHBV genomes were recloned into vector pTRE2-hyg under control of the TRE promoter. The vectors were transfected into tet-transactivator 2 (tTA2) containing HepG2.TA2-7 cells, and individual cell clones were selected using hygromycin. Clone DHBV-HA2/3_env- showed good inducibility of DHBV replication on Dox withdrawal and was used for all further experiments. (C) Kinetics of cccDNA formation in induced DHBV-HA2/3 cells. After the indicated times in Dox-free medium (6-well format) cells were harvested and nuclear viral DNAs extracted using the QIAamp DNA mini kit were subjected to southern blotting as in (B); postnuclear lysis each sample was supplemented with 150 pg pCD16 plasmid as recovery control. maintenance of the HA sequence in cccDNA was confirmed by sequencing of the PCR amplicon generated from nuclear DNA using DHBV primers D26832+ (corresponding to DHBV16 positions 2178–2200) / D26814- (complementary to positions 71–95). In parallel, duplicate aliquots (200 µL each) from the culture supernatants of the cells were examined by sandwich ELISA using anti-DHBc/e coated plates plus a rat monoclonal anti-HA antibody - peroxidase conjugate (Roche #12013819001) for detection. (D) Detection of HA-DHBeAg and DHBcAg by if 19 days after Dox withdrawal in HA2/3 cells using specific antibodies. Nuclei were stained with DAPI. (E) Effect of *POLK* silencing on HA-DHBeAg secretion in HA2/3 cells. HA2/3 cells were plated in absence of Dox and transduced with lentivirus encoding three different shRNAs targeting Polk. 3 days after transduction, cells were lysed, total RNA was extracted and *POLK* expression was quantified by RT-qPCR. Results are expressed as means±SD% relative *POLK* expression compared with shCtrl (set at 100%) from two biological replicates. In parallel, supernatant from POLK-silenced cells were harvested 21 days post Dox withdrawal and HA-DHBeAg secretion was quantified by anti-HA ELISA. Results are expressed as means±SD% relative HA-HBeAg secretion compared with shCtrl (set at 100%) from four independent experiments. cccDNA, covalently close circular DNA; DHBV, duck hepatitis B virus; HA, haemagglutinin.

the very weak intracellular HA-staining suggests that the tagged DHBeAg is efficiently secreted (figure 2D).

Notably, the time it takes for cccDNA and DHBeAg to exceed the lower limit of detection correlates with the scale of the experiment; for instance, one well of a 6-well plate (as used here) holds about 20-fold more cells than one well of 96-well plate (as used in the shRNA screen). For the screening in 96-well format we therefore established a more sensitive chemiluminescent ELISA format whereby the increase in HA signal became evident from around day 14 to day 22 postinduction. As an adequately enduring silencing of host factors by chemical siRNAs did not appear feasible, we instead went for a lentiviral shRNA expression approach. Optimisation with the screening platform determined that D21 was an appropriate time point for the analysis of gene silencing impact on HA-DHBeAg. For validation, we transduced HA2/3 cells with lentiviruses encoding three different validated shRNAs targeting the expression of *POLK* which was previously described as an important contributor to the formation of HBV cccDNA,[10] or a scrambled shRNA control. All three shRNAs achieved an approximately 80% reduction in *POLK* expression after 3 days (figure 2E), and this correlated with 40%–60% lower signals in the HA ELISA than in the shCtrl sample (figure 2E) 21 days after Dox withdrawal. Together these data indicated that the HA2/3 cell line is a relevant model to study cccDNA formation and regulation through the quantification of secreted DHBeAg, and hence is suited for

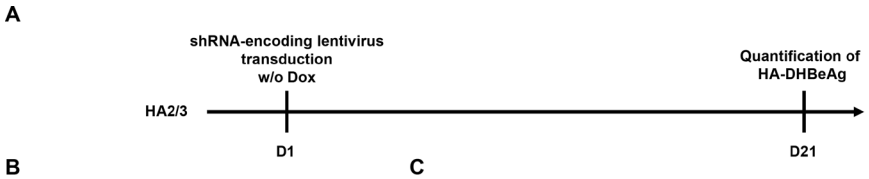

B

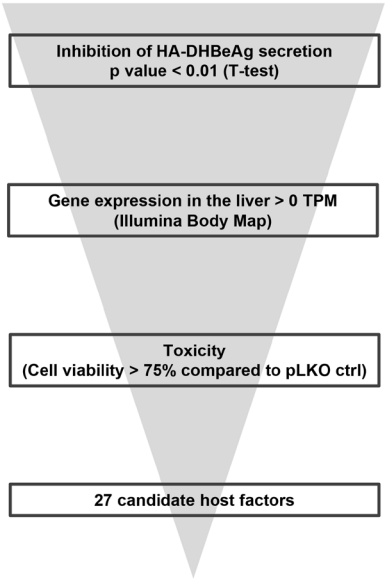

C

Gene	HA-HBeAg (% relative to pLKO)			Cell viability (% relative to pLKO)		Expression in the liver (TPM)
	Mean	SD	p-value	Mean	SD	
YBX1	25.2%	20.1%	2.6E-17	106.36%	9.0%	289.0
DUT	26.1%	8.4%	4.1E-23	77.98%	20.0%	7.0
CCNH	31.4%	13.0%	7.6E-16	102.26%	9.9%	9.0
RAD23B	31.7%	4.7%	2.2E-10	90.95%	6.1%	113.0
POLK	40.5%	24.0%	2.2E-22	97.33%	4.9%	3.0
FAAP24	45.2%	25.1%	2.2E-09	94.10%	2.4%	0.6
DDX11	47.3%	12.0%	2.4E-08	95.05%	6.0%	1.0
RAD51C	47.6%	23.3%	2.0E-09	99.50%	12.0%	2.0
HMGB1	47.7%	9.1%	7.8E-08	90.16%	13.0%	42
RAD9A	48.2%	12.9%	3.3E-08	97.35%	2.2%	2.0
EME1	48.7%	9.2%	1.6E-06	92.21%	4.8%	0.1
RAD21	49.1%	11.4%	1.5E-07	96.85%	7.3%	30.0
NABP1	49.2%	18.7%	5.4E-08	99.03%	2.8%	2.0
TDP2	49.7%	27.1%	3.5E-06	81.20%	28.6%	24.0
CHEK2	51.1%	25.3%	3.1E-10	93.15%	8.8%	0.8
SEM1	52.7%	12.2%	1.5E-05	94.88%	7.9%	12.0
SMC1A	53.4%	27.1%	2.0E-08	95.70%	5.7%	11.0
REV1	53.7%	41.4%	1.2E-07	84.76%	23.9%	3.0
POLG	54.8%	19.1%	4.6E-10	98.16%	3.6%	8.0
RAD17	56.9%	40.3%	1.2E-11	98.68%	2.8%	7.0
HMGB2	57.0%	22.3%	5.3E-15	99.35%	3.8%	7.0
GTF2H1	58.2%	15.6%	3.3E-12	98.98%	3.2%	6.0
RRM2B	59.3%	26.0%	6.0E-12	90.05%	9.9%	9.0
MBD4	59.6%	25.4%	1.1E-13	99.65%	6.9%	19.0
FEN1	60.0%	23.9%	1.5E-18	94.19%	7.5%	7.0
SMC3	60.2%	31.4%	8.2E-15	90.32%	7.6%	13.0
FANCL	60.2%	16.3%	8.2E-15	89.16%	14.8%	9.0

Figure 3 Approach of loss-of-function screen (LOF) in HA2/3 cells for the identification of HBV cccDNA host-dependancy factors. A. schematic workflow of LOF-screen. (B) Selection of candidate genes from the primary screen with the phenotypic robustness between replicates, the expression in the liver (illumina body MAP) and the toxicity (cell viability >75% compared with pLKO ctrl). (C) 27 candidates from the primary screen. The global effect of individual gene silencing on HBeAg production was analysed by pooling the effect of the three-independent shRNA per gene (n=9). P values were obtained through a two-tailed Student's t-test comparing phenotypic effects of shRNAs and pLKO ctrl. *POLK*, *TDP2* and *FEN1* are highlighted in blue. cccDNA, covalently close circular DNA; FEN1, flap endonuclease 1; HA, haemagglutinin; HBV, hepatitis B virus.

the identification of cccDNA-related host factors through RNAi-based loss-of-function screening.

A loss-of-function screen targeting the DNA damage response (DDR) machinery uncovers 27 candidate HBV cccDNA host-dependency factors

Given the anticipated crucial role of DNA repair in cccDNA formation, we next devised a lentiviral shRNA library targeting 239 genes belonging to the DNA damage response (DDR) machinery, with each gene being targeted by three independent shRNAs (online supplemental table S1). shRNAs targeting *POLK* expression were additionally used as positive controls, while empty pLKO vector and turboGFP expression vectors were used as negative controls. We then applied this targeted shRNA screen to the HA2/3 cell line, using as readout the HA-tagged DHBeAg ELISA values at 21 days after doxycycline withdrawal (figure 3A). Long-term silencing efficacy induced by shRNA was assessed by quantification of gene expression for one target (online supplemental figure S1). Using this approach, we identified a series of HBV cccDNA host factor candidates in which shRNA transduction correlated with a significant decrease in HA-DHBeAg production (figure 3B and online supplemental table S2). Computational analysis of the candidates including phenotypic variability and significance between replicates, toxicity and expression in the liver resulted in a short list of 27 candidates. Importantly, they included *POLK*, *TDP2* and *FEN1*, previously described as cccDNA-related HBV host factors, supporting the validity of our approach to uncover cccDNA host-dependency factors (figure 3C). Among the top-scoring candidates was *YBX1*, encoding the Y box binding protein 1 (formerly YB-1), also known as nuclease-sensitive element-binding or Y-box transcription factor. YBX1 is a DNA/RNA binding protein involved in several cellular processes, including DNA repair, regulation of transcription and translation, pre-mRNA splicing and mRNA packaging, that is, formation of mRNA nucleoprotein complexes.[19] Another top candidate was the DUT encoding deoxyuridine triphosphatase, a key enzyme of nucleotide metabolism which hydrolyzes dUTP to dUMP and pyrophosphate. DUT is an essential enzyme for maintaining DNA integrity by preventing misincorporation of uracil into DNA, which results in DNA toxicity and cell death.[20] Interestingly, dUTPase enzymes are encoded by many retroviruses and were shown to be essential for viral replication of HIV types 1 and 2.[20] As a pararetrovirus expressing no dUTPase, endogenous dUTPase may well play an important role in the life cycle of HBV by preserving the integrity of viral DNA. Yet another top-scorer was *DDX11* which encodes a DEAD box DNA helicase (DDX11) involved in DNA replication recovery from DNA damage.[21] An early step in cccDNA conversion from rcDNA is the removal of protein P and the RNA oligomer from the 5' ends of the two DNA strands. Removal of the respective flap-structures has been ascribed to FEN1 which is also one of the five core factors for *in vitro* cccDNA formation.[12] DDX11 cooperates with FEN1 during removal of 5'-flap structures during Okazaki fragment maturation and long-patch base excision repair.[22]

Taken together, our approach enabled to uncover several previously unidentified cccDNA-related host factor candidates. Given the HBV infection phenotype on silencing, absent or at most limited host cell toxicity during silencing, high expression in the liver (figure 3C) and previously described targetability by small molecules[23 24] we chose to focus on YBX1 for further analyses. In this context, we first confirmed by Southern blot the effect of YBX1 and POLK depletion on human HBV cccDNA levels in another reporter cell line, HAC18, which expresses the HBV genome in an analogous manner to the DHBV genome in HA2/3 cells (online supplemental figure S2).

Validation of YBX1 as an HBV host factor in an HepG2-NTCP cell infection model

Next, we aimed to validate the role of YBX1 in state-of-the-art HBV infection models. Taking advantage of our previously described HepG2-NTCP cell line susceptible to robust HBV-infection,[25] we performed silencing studies using shRNA targeting *YBX1* expression. HepG2-NTCP were individually transduced with three different shRNA-containing lentivirus constructs, selected with puromycin 48 hours prior to HBV infection and harvested 10 days postinfection (figure 4A). While *TDP2*-knock-out (KO) cells have been reported to be permissive to HBV infection,[26] DHBV cccDNA accumulation was slowed down in these cells.[26] Moreover, *TDP2* was identified as a target in our primary screen. Consequently, *TDP2*-targeting shRNA was used as a control. Knockdown of both *TDP2* and *YBX1* resulted in a marked reduction of secreted HBeAg, intracellular HBV RNA (both pgRNA and PreC RNA (see online supplemental table S3) and intracellular HBsAg levels (figure 4B–D), revealing a significant decrease in HBV infection in *YBX1*-silenced HepG2-NTCP cells.

We then generated *YBX1*-KO HepG2-NTCP cells using CRISPR-Cas9 technology (figure 4E) and specific guide RNA. A robust decrease in YBX1 expression was observed in cells transduced with sgRNA targeting *YBX1* (figure 4F). Functional analyses on infection with HBV showed a marked decrease in the levels of HBV markers in *YBX1*-KO HepG2-NTCP cells compared with HepG2-NTCP not related to cell viability (Figure 4G,H). Collectively, these functional analyses support an important role for YBX1 in HBV infection of HepG2-NTCP cells.

To study the functional role of YBX1 for the formation and/or maintenance of HBV cccDNA levels, we assessed HBV DNA replication intermediates in HBV infected *YBX1*-silenced HepG2-NTCP cells by Southern blot. As shown in figure 4I and figure 4J, shRNA-induced silencing of *YBX1* resulted in a marked decrease in cccDNA levels relative to non-silenced HBV-infected cells. The identity of the band marked as cccDNA was confirmed by heat denaturation and subsequent linearisation by EcoRI digestion (online supplemental figure S3). Similar results were observed in HBV-infected *YBX1*-KO HepG2-NTCP cells (Figure 4I,J). Interestingly, no decrease in HBV infection was observed when *YBX1* knockdown in HBV-infected HepG2-NTCP cells was achieved after virus infection when the initial cccDNA pool is already established (online supplemental figure S4). Comparable results were observed in HA2/3 cells (online supplemental figure S4).

Finally, we aimed to clarify the mode of action by which YBX1 affects the early steps of the HBV life cycle. First, loss-of-function studies did not reveal a significant modulation of key cccDNA host factor expression on *YBX1* knockdown, including *POLK*, *TDP2* and *PCNA* (online supplemental figure S5A). Next, we functionally excluded a major role of YBX1 on viral cell entry, as no effect on infection of *YBX1*-KO Huh7-NTCP cells by hepatitis D virus was observed (online supplemental figure S5B-D) which, like HBV, uses NTCP as entry receptor. Taken together, these results confirm a key functional role of YBX1 in early steps of the HBV life cycle in infected hepatocytes, subsequent to virus entry but prior to the establishment of the initial cccDNA pool.

YBX1 is recruited to HBV DNA

The above results led us to hypothesise that due to its nucleic acid binding abilities,[19] YBX1 might directly interact with the HBV genome to promote cccDNA formation and accumulation. YBX1 is well known to bind to promoter/enhancer regions containing a Y-box motif (5'-CTGATTGGCCAA-3'),[27] although other DNA and RNA sequences can also be bound.[28] Moreover, it has been previously reported that YBX1 can bind to integrated HBV DNA regions.[29] Importantly, using sequence alignments as shown in figure 5A, we found putative Y-box motifs within the HBV ayw reference sequence (GenBank V01460.1) as well as within the DHBV16 reference sequence (GenBank K01834.1). Therefore, to investigate whether the YBX1-induced HBV regulation involves the recruitment of YBX1 to the HBV genome, we performed chromatin immunoprecipitation (ChIP) qPCR assays on nuclear extracts from HBV-infected HepG2-NTCP cells with an anti-YBX1 antibody and an anti-HBcAg antibody as a positive control (figure 5B). Immunoprecipitation efficacy was controlled by Western blot detection of the precipitated proteins (figure 5B). Importantly, ChIP-qPCR analysis revealed specific recruitment of YBX1 to HBV DNA in the nucleus of infected HepG2-NTCP cells (figure 5C). Notably, we confirmed this result using nuclear extracts from three HBV-infected chimeric FRG-NOD mice (online supplemental table S4) suggesting that this interaction is present during HBV infection *in vivo*, although the kinetics of this interaction in the context of cccDNA steady-state levels still remains to be determined, since the ChIP assays was performed at a single time point both in cell culture models and in chronically infected human chimeric mice (figure 5C,D).

The rescue of YBX1 expression in KO cells restores cccDNA formation and HBV infection

To validate the canonical association between YBX1 and HBV DNA, we took advantage of *YBX1*-KO HepG2-NTCP cells (figure 6A). We designed *YBX1* cDNA constructs carrying silent mutations in the sgRNA target sequence, and coding for the wild type amino acid sequence of YBX1 (YBX1-WT). We restored YBX1 expression in the *YBX1*-KO HepG2-NTCP cells, leading to robust and similar protein expression compared with endogenous levels (figure 6B). These cells were then infected by HBV. As shown in figure 6C, ectopic restoration of YBX1-WT was associated with a rescue of HBV infection phenotype, as measured by HBeAg secretion at day 10 postinfection. Importantly, YBX1-WT expression restored cccDNA levels at day 2 postinfection as shown by qPCR, confirming the importance of YBX1 in the early steps of the HBV life cycle and cccDNA formation or regulation (figure 6C). The increase in cccDNA levels in *YBX1*-KO cells expressing YBX1-WT was confirmed by Southern blot analyses (online supplemental figure S6). Finally, we performed ChIP-qPCR assays on nuclear extracts from HBV infected *YBX1*-KO cells expressing either YBX1-WT and confirmed the ability of the ectopic version of YBX1 to bind HBV DNA (figure 6E). Taken together, our results confirm the importance of YBX1 in the early steps of the viral life cycle and the early formation or regulation of cccDNA.

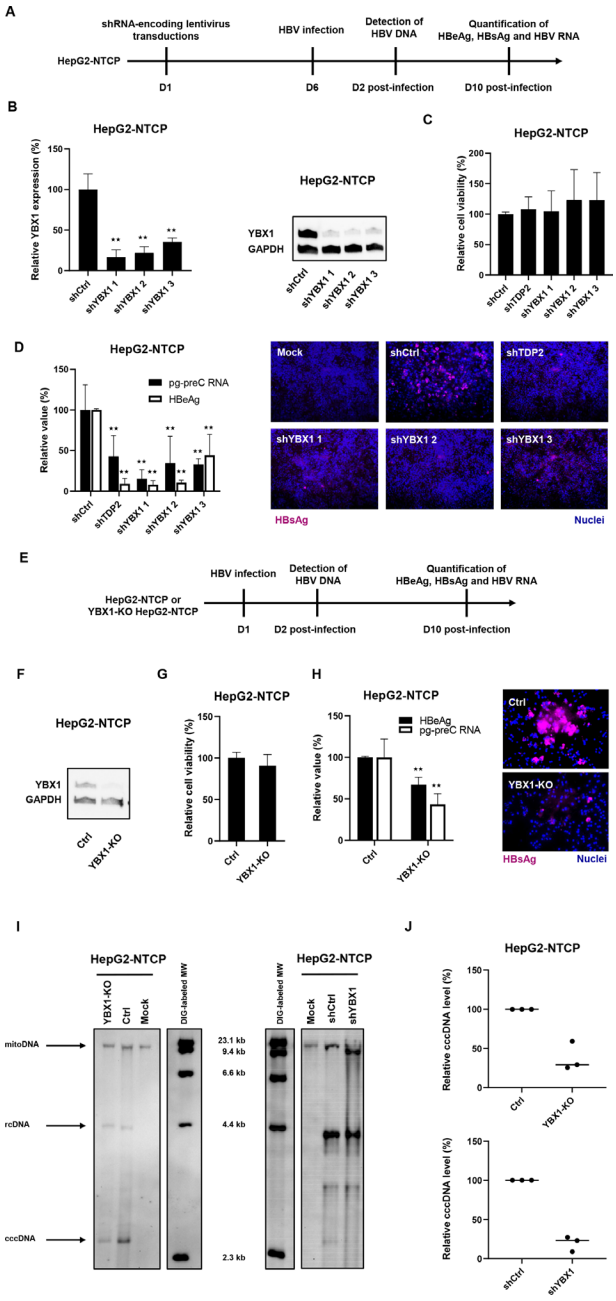

Figure 4 Validation of YBX1 as a HBV cccDNA host-dependency factor in the HBV permissive cell line HepG2-NTCP. (A) Experimental approach and timelines for the shRNA-based validation approach. HepG2-NTCP cells were transduced with lentivirus encoding three *YBX1*-targeting shRNA (shYBX1 1, 2, 3) 3 days post-transduction, total RNA was extracted and *YBX1* expression was quantified by RT-qPCR (B), left panel). Results are expressed as means±SD% relative *YBX1* expression compared with shCtrl (set at 100%) from three independent experiments. in parallel, *YBX1* expression was controlled by Western blot in transduced HepG2-NTCP (B), right panel). One representative blot is shown. 6 days post-transduction, cells were then infected with HBV. (C) Cell viability was assed 10 days postinfection (DPI). Results are expressed as means±SD% relative cell viability compared with shCtrl (set at 100%) from three independent experiments. (D) HBV infection was assessed by quantification of HBV markers at 10 DPI: secreted HBeAg by CLIA (white) and HBV pg-preC RNA by RT-qPCR (white). Results are expressed as means±SD% relative HBV infection compared with shCtrl (set as 100%) from three independent experiments. intracellular HBsAg expression was assessed by if 10 DPI. (E) Experimental approach and timelines for the CRISPR/Cas9 validation approach. *YBX1*-KO cell line was produced from HepG2-NTCP cells through CRISPR/Cas9 technology using a specific sgRNA targeting *YBX1*. (F) YBX1 protein expression in *YBX1*-KO cells compared with parental HepG2-NTCP cells (Ctrl) was assessed by Western blot. cells were then infected with HBV for 10 days G. cell viability was assessed 10 DPI. Results are expressed as means±SD% relative cell viability compared with HBV-infected HepG2-NTCP (set at 100%) from three independent experiments. (H) HBV infection was assessed 10 DPI by quantification of secreted HBeAg by CLIA (black) and HBV pg-preC RNA quantification by RT-qPCR (white). Results are expressed as means±SD% relative HBV infection compared with HBV-infected HepG2-NTCP (set as 100%) from three independent experiments. Intracellular HBsAg expression was assessed 10 dpi by if. (I) Detection of HBV DNAs by Southern blot from *YBX1*-silenced and *YBX1*-KO cells. HBV rcDNA and HBV cccDNA are indicated. One representative experiment is shown. (K) Quantification of cccDNA levels. cccDNA levels were quantified using ImageJ software. Three independent experiments are shown. **p<0.01 (two-tailed Mann-Whitney U test). cccDNA, covalently close circular DNA; HBV, hepatitis B virus; NTCP, sodium-taurocholate cotransporting polypeptide.

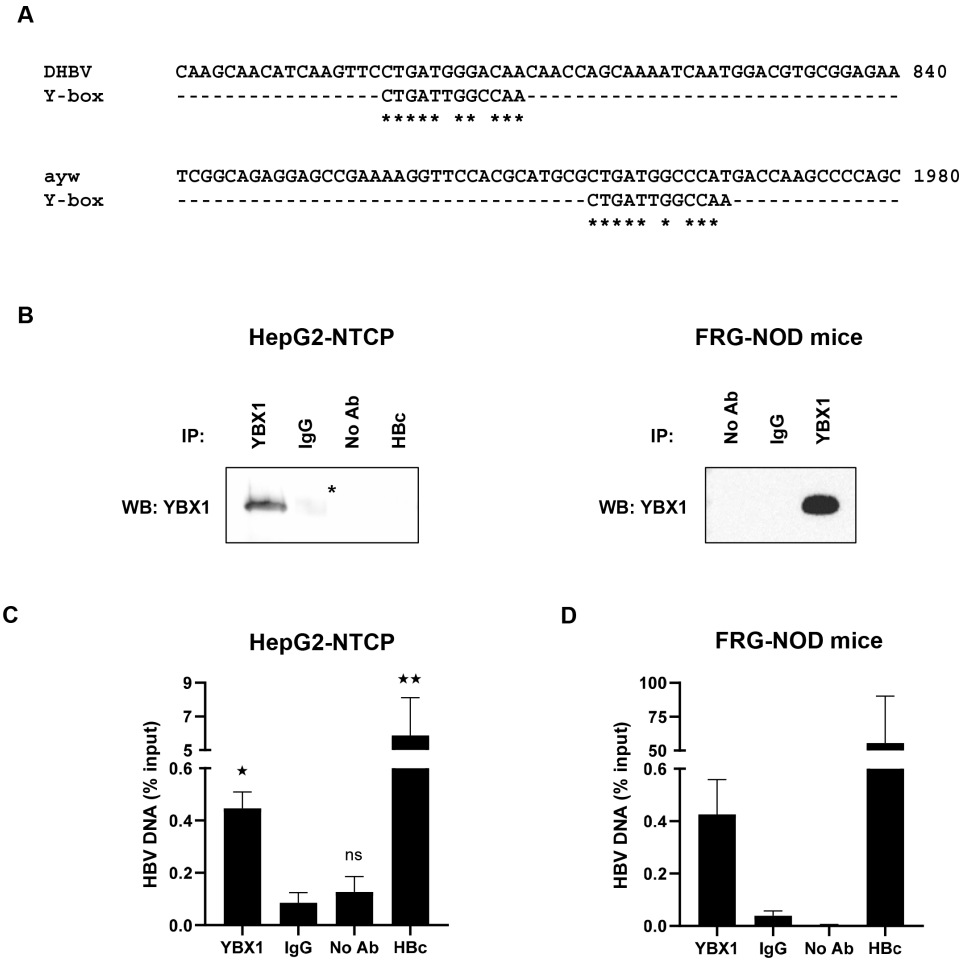

Figure 5 YBX1 binds to HBV DNA. (A) Putative Y-box motifs within the DHBV (K01834.1) and HBV genomes (ayw strain; V01460.1). (B, C). ChIP-qPCR assay on HBV-infected HepG2-NTCP cells. HepG2-NTCP cells were infected with HBV. nuclear DNA was extracted two DPI and CHIP was performed using a specific anti-YBX1 antibody and a specific anti-HBcAg (HBc) antibody as a positive control. Immunoprecipitation efficacy was assessed by Western blot (B). The StAR in the blot corresponds to non-specific signal due to the presence of heavy chains (around 50 kDa) from the rabbit isotype control used for the immunoprecipitation and that are still weakly detected despite the use of an adapted HRP reagent. HBV DNA in immunoprecipitated eluates was quantified by qPCR (C). Results are shown as means±SEM% HBV DNA in eluates compared with input samples from five biological replicates. (D) The same ChIP-qPCR assay was performed using nuclear extracts from HBV-infected FRG-NOD mice. Results are shown as means±SEM% HBV DNA in eluates compared with input samples from three independent mice (one sample per mouse). ⋆p<0.05; ⋆⋆p<0.01 (two-tailed Mann-Whitney U test). ChIP, chromatin immunoprecipitation; HBV, hepatitis B virus; NS, non-significant

Validation of functional role of YBX for the HBV life cycle in primary human hepatocytes

We next validated the functional role of YBX1 for the HBV life cycle in primary human hepatocytes, the *in vitro* model most closely related to HBV infection in patients (figure 7A). Silencing of *YBX1* expression in PHH prior to HBV resulted in a marked decrease in HBeAg secretion and cccDNA levels (figure 7B–E). These data confirm in the clinically most translatable HBV infection cell-based model a functional role of YBX1 in the HBV life cycle. Of note, *YBX1* expression was upregulated in HBV-infected PHH compared with non-infected cells (figure 7F).

Analysis of *YBX1* gene expression in patients with chronic HBV infection and liver disease

Based on our observation that HBV can modulate *YBX1* expression in PHH (figure 7F), we next studied *YBX1* gene expression in liver tissues in different cohorts of patients with HBV infection and liver disease. As controls we used hepatitis C virus (HCV)-infected or NASH patients with a similar disease phenotype.

A significant positive correlation (Spearman's r=0.85, p=0.006) was observed between HBV viral load and *YBX1* expression in liver tissues from nine HBV-infected patients (GSE14322) (figure 8A),[25] suggesting that YBX1 may be a clinically relevant factor for HBV infection.[30] Indeed, higher expression of *YBX1* in the livers from patients with surgically resected HBV-related HCC was associated with significantly higher probability of tumour recurrence after the resection (figure 8B) and eventually lower long-term overall survival rate (figure 8C). Furthermore, we observed a marked and significant correlation between *YBX1* expression and the expression of fibrosis-associated genes, including VIM, encoding the vimentin in HBV-infected patients (GSE121248) (Spearman's r=0.60/p = 8.332e-05) (figure 8D). Vimentin is a well-described biomarker for several cancers including sarcoma,[31] known to be involved in the progression of liver disease and HCC.[32]

In contrast, there were no significant associations with fibrosis progression in a cohort of NASH patients (GSE49541) or HCV load, although a non-significant positive tendency was observed

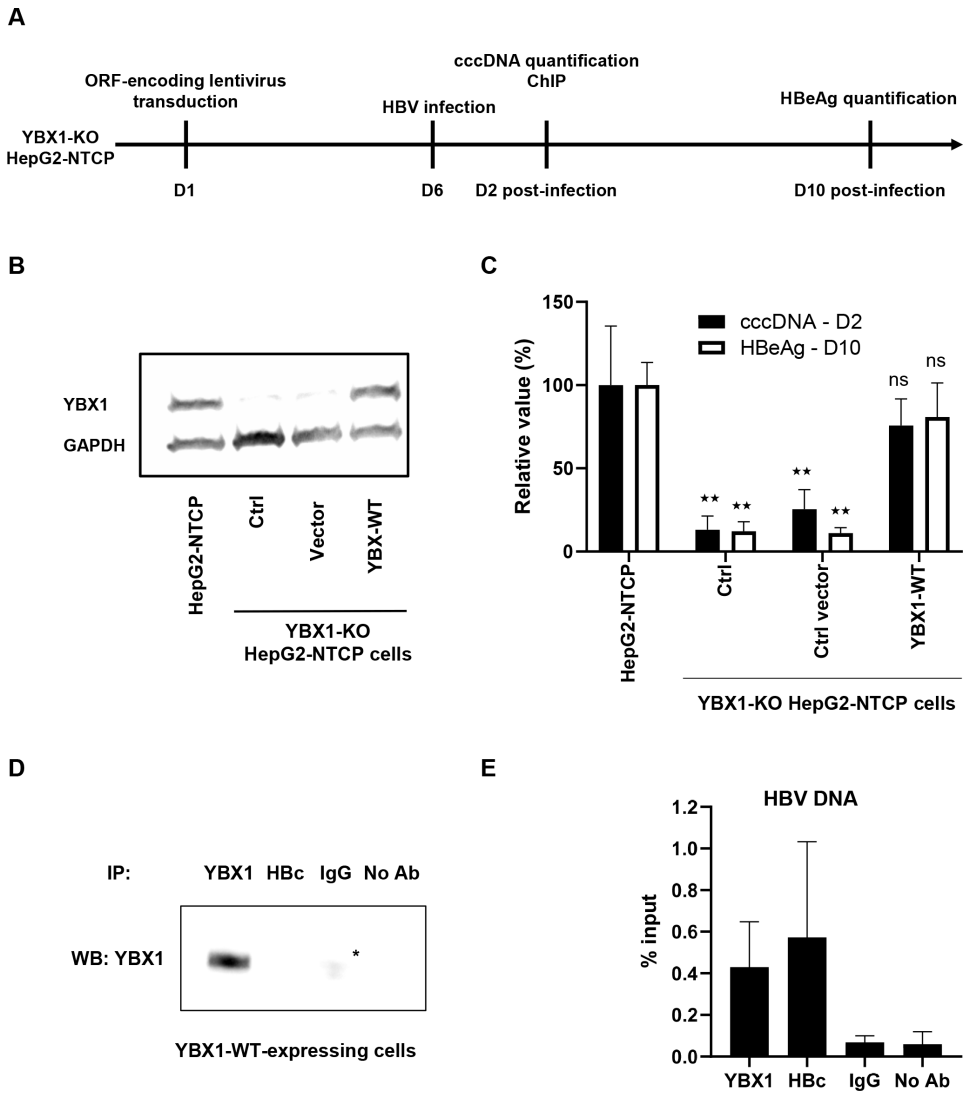

Figure 6 Rescue of YBX1 expression restores HBV infection in *YBX1*-KO cells. (A) Experimental timelines. *YBX1*-KO cells were transduced with lentivirus encoding the wild type version of YBX1 (YBX1-WT). (B) YBX1 expression was controlled by Western blot. 6 days after transduction, cells were infected by HBV. Two days postinfection, DNA was extracted and cccDNA levels were quantified by specific qPCR (C). Results are expressed as means±SD% relative cccDNA levels secretion compared with HepG2-NTCP cells (set as 100%) from three independent experiments. in parallel, secreted HBeAg levels were quantified 10 DPI by CLIA. Results are expressed as means±SD% relative HBeAg secretion compared with HepG2-NTCP cells (set as 100%) from three independent experiments (C–E). In parallel, ChIP-qPCR assay was performed on YBX1-WT-expressing HepG2-NTCP cells infected by HBV at day two postinfection using a specific anti-YBX1 antibody, a specific anti-HBc antibody, or a control IgG. YBX1 immunoprecipitation efficiency was assessed by Western blot (D). The StAR in the blots correspond to non-specific signal due to the presence of heavy chains (around 50 kDa) from the rabbit isotype control used for the immunoprecipitation (E). Results are expressed means±SDM HBV DNA levels (% input) from three biological replicates. ★★p<0.01 (two-tailed Mann-Whitney U test). cccDNA, covalently close circular DNA; ChIP, chromatin immunoprecipitation; HBV, hepatitis B virus; KO, knock-out; NS, non-significant; NTCP, sodium-taurocholate cotransporting polypeptide.

between *YBX1* expression and disease progression and survival in patients with HCV-related cirrhosis (GSE15654) (figure 8E–H).

DISCUSSION

In this study, we established a novel cell-based reporter assay using a simple ELISA as a readout which enables fast-track discovery of HBV cccDNA host factors as antiviral targets for cure. Using this assay, we identified YBX1 as a previously undiscovered HBV host-dependency factor. Moreover, gene expression analyses in patients suggest that YBX1 is clinically not only relevant for the HBV life cycle but also for the pathogenesis of virus-induced liver disease and cancer.

A key limitation for the investigation of cccDNA formation is the low number of cccDNA copies in infected cells. The cell-based reporter system described in this study overcomes this challenge by enabling the non-invasive monitoring of cccDNA via the cccDNA-dependent generation of a secreted HA tagged DHBeAg. We note that Cai *et al* independently described a principally similar system for HBV.[33] In our study, we decided to initially focus on DHBV, a hepadnavirus closely related to HBV, because it produces a much higher number of cccDNA copies per cell compared with human HBV even in the same human hepatoma cells.[8] This approach can be scaled up to 96 or 384 well plates allowing medium-sized drug or loss-of-function screens. The ELISA format allows simple automatic or robotic analyses.

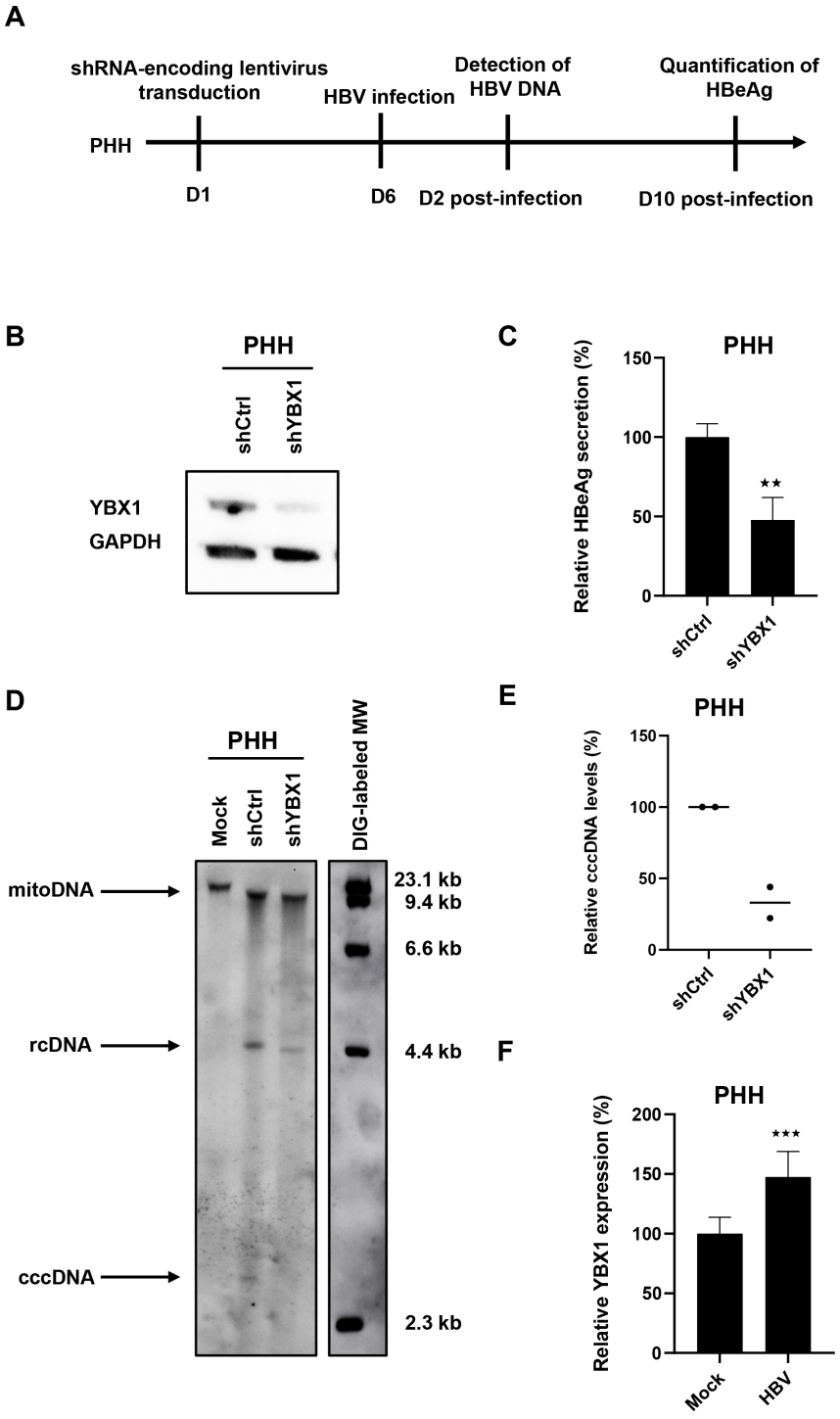

Figure 7 Ybx1 knock-down inhibits HBV infection in primary human hepatocytes. (A) Experimental approach and timelines. Primary human hepatocytes (PHH) cells were transduced with lentivirus encoding a *YBX1*-targeting shRNA (shYBX1) 3 days post-transduction, YBX1 expression was controlled by Western blot. (B) One representative blot is shown. Six days post-transduction, PHH cells were then infected with HBV, and HBV infection was assessed by quantification of secreted HBeAg by CLIA 10dpi. Results are expressed as means±SD% relative HBV infection compared with shCtrl (set as 100%) from three independent experiments. (C) In parallel, PHH cells were lysed at day 2 postinfection, DNA was extracted and HBV DNA was detected by Southern blot (D). HBV rcDNA and HBV cccDNA are indicated. One representative experiment is shown. (E) Quantification of cccDNA levels using ImageJ software from two independent experiments. (F) *YBX1* mRNA expression in HBV-infected PHH. PHH were infected with HBV and *YBX1* expression was assessed 10 dpi. Results are expressed as means±SD% relative *YBX1* expression compared with shCtrl (set at 100%) from four independent experiments. ** p<0.01; *** p<0.01 (two-tailed Mann-Whitney U test). cccDNA, covalently close circular DNA; HBV, hepatitis B virus; RCdna, relaxed circular dna.

The inter-assay reproducibility is high, thus minimising the need for many replicates or repetitions. The assay is fast with robust read-outs in 2 weeks. These features provide a major conceptual and technical advance compared with current assays requiring RT-PCR or blotting approaches. While the biology of duck and human cccDNA is similar, it is notable that differences may

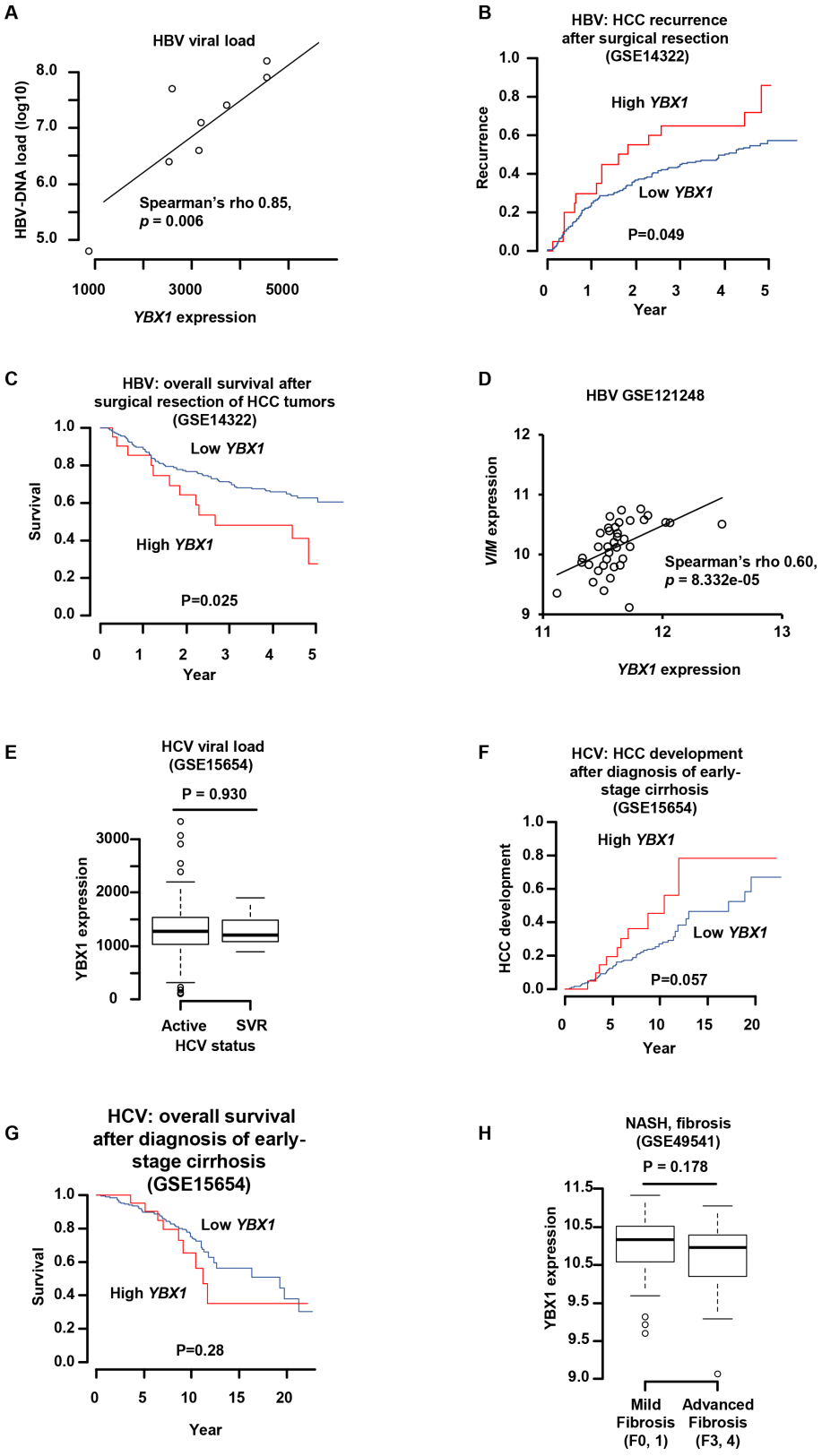

Figure 8 *YBX1* expression correlates with HBV load, HCC recurrence and survival in patients. (A) *YBX1* mRNA expression in HBV-infected patients (cohort described in methods). (B, C) Tumour recurrence (B) and survival (C) and level of *YBX1* expression (low-high) in a cohort of HBV-induced HCC patients (GSE14322). (D) Correlation between *YBX1* expression and *VIM* expression in HBV-infected patients (GSE121248). (E) Correlation between *YBX1* expression and the NASH fibrosis stage (GSE49541). (F) Correlation between *YBX1* expression and the HCV status. (G, H) Survival (G) and HCC development (H) depending on level of *YBX1* expression (low-high) (GSE15654). HBV, hepatitis B virus; HCC, hepatocellular carcinoma; HCV, hepatitis C virus.

exist in cccDNA formation between DHBV and HBV, as already suggested by the much higher cccDNA levels DHBV can accumulate in the same cells[8] and DHBV's apparently more pronounced dependence on TDP2.[9 26] However, the identification of known HBV cccDNA-dependency factors beyond TDP2 such as POLK, and FEN1 confirms the ability of our approach to use DHBV cccDNA as a template to identify HBV cccDNA-related host factors. Furthermore, we have developed an HA2/3 analogous HBV cell line with cccDNA dependent HA-HBeAg production (HAC18) in which we could confirm the negative impact of YBX1 depletion (online supplemental figure S2). However, the high cccDNA levels in HA2/3 cells remain a major technical advantage because they also correlate with higher HA-ELISA signals. We note that HA-HBeAg secretion in our assay would respond not only to alterations in the multiple steps of cccDNA formation and/or transcription from the cccDNA minichromosome, but also to factors involved in translation of the precore protein and/or its processing and secretion as HBeAg. Our choice of anti-DDR shRNAs makes the latter scenario unlikely for the current study yet also opens additional future opportunities.

Using this approach, we identified YBX1 as a previously undiscovered HBV host-dependency factor, although not essential for cccDNA production as it is not totally abolished in *YBX1*-KO cells (figure 4). The functional relevance of YBX1 for the HBV life cycle was confirmed by several lines of evidence: (1) Genetic *YBX1* loss-of-function analyses using CRISPR-Cas9 or shRNA resulted in a marked decrease in HBV infection in cell lines and primary human hepatocytes. (2) A substantial reduction in cccDNA levels confirmed functional relevance of YBX1 to synthesise and maintain robust cccDNA levels. (3) A specific recruitment of YBX1 to HBV genome. YBX1 is a multifunctional DNA/RNA-binding protein that regulates transcription and translation.[19] Increased levels of YBX1 have been correlated with DNA topoisomerase II activity, already described as cccDNA-related HBV host factor. Moreover, a previous study reported a direct interaction between YBX1 and PCNA,[34] one of the crucial factors required for *in vitro* cccDNA formation.[12] Although we do not observe a modulation of PCNA expression on *YBX1* silencing (online supplemental figure S5), a detailed understanding of the functional role of YBX1-PCNA interaction in cccDNA formation would require additional studies. Collectively, our data indicate events after entry and preceding establishment of the cccDNA pool as major target(s) for YBX1 proviral activity. However, further studies are needed to unravel in more detail the molecular mechanism(s) of YBX1 in cccDNA formation and/or regulation in the HBV life cycle. YBX1 is a targetable protein and therefore a candidate for antiviral therapy. Small molecules specifically targeting YBX1 should be tested to assess its potential as an antiviral target. Although several YBX1-targeting drugs have been described, such as fisetin[23] or CYT387,[24] they have additional targets beyond YBX1.[24 35 36] YBX1-specific specific inhibitors would be required to further confirm the targetability of YBX1 using a small molecule approach.

Since YBX1 is involved in the modulation of several signal transductions pathways, HBV-YBX1 interaction may also play a role in the pathogenesis of virus-induced liver disease and HCC. Indeed, in patients, *YBX1* expression is accompanied by expression of genes involved in liver disease progression, as well as lower survival of HCC patients. High expression of *YBX1* is often detected in various cancers including HCC, and is closely related to the progression, poor prognosis and multidrug resistance.[37 38] In this regard it is also of interest to note that YBX1 has been suggested as target in anticancer therapies.[39] However, additional experiments are required to fully evaluate the functional role of HBV in the regulation of *YBX1* expression and disease biology.

Collectively, the implication of our study is threefold: (1) We have established a robust and simple cell-based system enabling to discover HBV cccDNA-dependency factor as targets for viral cure; (2) our study uncovers the DNA repair factor YBX1 as an important factor for cccDNA biology, providing an opportunity for exploring YBX1 as target for HBV cure; (3) we observed an association between HBV infection, *YBX1* expression and virus-induced liver disease suggesting that targeting YBX1 may not only reduce viral cccDNA but potentially also ameliorate HBV-induced liver disease and cancer incidence.

MATERIALS AND METHODS

All the materials, reagents and protocols are detailed in online supplemental material.

Author affiliations
[1]Université de Strasbourg, Inserm, Institut de Recherche sur les Maladies Virales et Hépatiques UMRS 1110, Strasbourg, France
[2]Department of Internal Medicine II/Molecular Biology, University Hospital Freiburg, Freiburg, Germany
[3]IGBMC, Plateforme de Criblage Haut-débit, Illkirch, France
[4]Department of Internal Medicine, Liver Tumor Translational Research Program, Simmons Comprehensive Cancer Center, Division of Digestive and Liver Diseases, University of Texas Southwestern Medical Center, Dallas, Texas, USA
[5]Department of Gastroenterology and Hepatology, Chang Gung Memorial Hospital, Taoyuan, Taiwan
[6]Broad Institute of Massachusetts Institute of Technology and Harvard, Cambridge, Massachusetts, USA
[7]Institut Hospitalo-Universitaire, Pôle Hépato-digestif, Nouvel Hôpital Civil, Strasbourg, France

Twitter Eloi R Verrier @eloi_verrier

Acknowledgements We thank our colleagues Sarah Durand (Inserm UMR_S1110, Strasbourg, France), Elodie Boeuf and Amélie Weiss (IGBMC, Illkirch-Graffenstaden, France), and Céline Costa (University of Freiburg, Germany) for excellent technical support. Joachim Lupberger and Karim Majzoub (Inserm UMR_S1110, Strasbourg, France) for helpful discussions. We thank our collaborator Julie Lucifora (CIRI, Lyon, France) for excellent technical support on ChIP assays.

Contributors TB is the guarantor of the study and serves as lead corresponding author. TB and MN initiated the study, designed and supervised research. ERV, LH, KD, JM, MN and TB produced and characterised the HA2/3 cell line. ERV, AM-R, LB, MN and TB set up, designed and performed the shRNA screen. ERV and GL analyzed the screen. GL and LH performed the validation experiments with the support of MJH and AM. EF and PP provided human hepatocytes. LM provided mouse samples. ERV, GL, LH, CS, AM, MJH, LM, MN and TB analysed the data. ERV, GL, FJ, HES, NF, S-YH, YH and TB analyzed the clinical data. ERV, GL, MN and TB wrote the manuscript. All the authors read and edited the manuscript. ERV and GL contributed equally as first authors. MN and TB contributed equally to this work as senior authors. All the authors approved the study.

Funding This work was supported by Inserm, the University of Strasbourg, the European Union (Infect-ERA hepBccc, ERC-2014-AdG-671231-HEPCIR, ERC-AdG-2020-FIBCAN #101021417 and Horizon 2020 research and innovation programme under grant agreement 667273 - HEPCAR), Agence Nationale de Recherches sur le Sida et les Hépatites Virales (ANRS ECTZ87384) and the French Cancer Agency (ARC IHU201901299). This work of the Interdisciplinary Thematic Institute IMCBio, as part of the ITI 2021-2028 program of the University of Strasbourg, CNRS and Inserm, was supported by IdEx Unistra (ANR-10-IDEX-0002), and by SFRI-STRAT'US project (ANR 20-SFRI-0012) and EUR IMCBio (ANR-17-EURE-0023) under the framework of the French Investments for the Future Program. GL is the recipient of an ANRS fellowship (ECTZ86820 and ECTZ158023). ERV acknowledges fundings from ANRS (ECTZ104527), and the French National Research Agency (ANR, grant number ANR-21-CE15-0035-01 DELTArget).

Competing interests None declared.

Patient and public involvement Patients and/or the public were not involved in the design, or conduct, or reporting, or dissemination plans of this research.

Patient consent for publication Not applicable.

Ethics approval Primary human hepatocytes (PHH) were obtained from liver tissue from patients undergoing liver resection for liver metastasis at the Strasbourg University Hospitals with informed consent. Protocols were approved by the local

Ethics Committee of the Strasbourg University Hospitals (CPP) and the Ministry of Higher Education and Research of France (DC 2016 2616). Human samples from HBV infected patients followed at the Chang Gung Memorial Hospital (Taipei, Taiwan) were obtained with informed consent. Protocols were approved by the local Ethics Committee (Institutional Review Board 102-3825C). Participants gave informed consent to participate in the study before taking part.

Provenance and peer review Not commissioned; externally peer reviewed.

Data availability statement Data are available on reasonable request. All data relevant to the study are included in the article or uploaded as online supplemental information. .

ORCID iDs
Gaëtan Ligat http://orcid.org/0000-0003-1237-1936
Naoto Fujiwara http://orcid.org/0000-0002-4109-3421
Catherine Schuster http://orcid.org/0000-0001-7281-4511
Michael Nassal http://orcid.org/0000-0003-2204-9158
Thomas F. Baumert http://orcid.org/0000-0002-8864-2168

REFERENCES

1 Llovet JM, Zucman-Rossi J, Pikarsky E, *et al*. Hepatocellular carcinoma. *Nat Rev Dis Primers* 2016;2:16018.
2 Ginzberg D, Wong RJ, Gish R. Global HBV burden: guesstimates and facts. *Hepatol Int* 2018;12:315–29.
3 Ligat G, Goto K, Verrier E, *et al*. Targeting viral cccDNA for cure of chronic hepatitis B. *Curr Hepatol Rep* 2020;19:235–44.
4 Nassal M. Hepatitis B viruses: reverse transcription a different way. *Virus Res* 2008;134:235–49.
5 Summers J, O'Connell A, Millman I. Genome of hepatitis B virus: restriction enzyme cleavage and structure of DNA extracted from Dane particles. *Proc Natl Acad Sci U S A* 1975;72:4597–601.
6 Herrscher C, Roingeard P, Blanchard E. Hepatitis B virus entry into cells. *Cells* 2020;9. doi:10.3390/cells9061486. [Epub ahead of print: 18 Jun 2020].
7 Nassal M. Hbv cccDNA: viral persistence reservoir and key obstacle for a cure of chronic hepatitis B. *Gut* 2015;64:1972–84.
8 Köck J, Rösler C, Zhang J-J, *et al*. Generation of covalently closed circular DNA of hepatitis B viruses via intracellular recycling is regulated in a virus specific manner. *PLoS Pathog* 2010;6:e1001082.
9 Königer C, Wingert I, Marsmann M, *et al*. Involvement of the host DNA-repair enzyme TDP2 in formation of the covalently closed circular DNA persistence reservoir of hepatitis B viruses. *Proc Natl Acad Sci U S A* 2014;111:E4244–53.
10 Qi Y, Gao Z, Xu G, *et al*. DNA polymerase κ is a key cellular factor for the formation of covalently closed circular DNA of hepatitis B virus. *PLoS Pathog* 2016;12:e1005893.
11 Kitamura K, Que L, Shimadu M, *et al*. Flap endonuclease 1 is involved in cccDNA formation in the hepatitis B virus. *PLoS Pathog* 2018;14:e1007124.
12 Wei L, Ploss A. Core components of DNA lagging strand synthesis machinery are essential for hepatitis B virus cccDNA formation. *Nat Microbiol* 2020;5:715–26.
13 Schreiner S, Nassal M. A role for the host DNA damage response in hepatitis B virus cccDNA Formation-and beyond? *Viruses* 2017;9:125.
14 Sun D, Nassal M. Stable HepG2- and Huh7-based human hepatoma cell lines for efficient regulated expression of infectious hepatitis B virus. *J Hepatol* 2006;45:636–45.
15 Cai D, Mills C, Yu W, *et al*. Identification of disubstituted sulfonamide compounds as specific inhibitors of hepatitis B virus covalently closed circular DNA formation. *Antimicrob Agents Chemother* 2012;56:4277–88.
16 Nassal M, Rieger A. An intramolecular disulfide bridge between CYS-7 and CYS61 determines the structure of the secretory core gene product (E antigen) of hepatitis B virus. *J Virol* 1993;67:4307–15.
17 DiMattia MA, Watts NR, Stahl SJ, *et al*. Antigenic switching of hepatitis B virus by alternative dimerization of the capsid protein. *Structure* 2013;21:133–42.
18 Bardens A, Döring T, Stieler J, *et al*. Alix regulates egress of hepatitis B virus naked capsid particles in an ESCRT-independent manner. *Cell Microbiol* 2011;13:602–19.
19 Lyabin DN, Eliseeva IA, Ovchinnikov LP. Yb-1 protein: functions and regulation. *Wiley Interdiscip Rev RNA* 2014;5:95–110.
20 Hizi A, Herzig E. dUTPase: the frequently overlooked enzyme encoded by many retroviruses. *Retrovirology* 2015;12:70.
21 Shah N, Inoue A, Woo Lee S, *et al*. Roles of ChlR1 DNA helicase in replication recovery from DNA damage. *Exp Cell Res* 2013;319:2244–53.
22 Farina A, Shin J-H, Kim D-H, *et al*. Studies with the human cohesin establishment factor, ChlR1. Association of ChlR1 with Ctf18-RFC and FEN1. *J Biol Chem* 2008;283:20925–36.
23 Khan MI, Adhami VM, Lall RK, *et al*. YB-1 expression promotes epithelial-to-mesenchymal transition in prostate cancer that is inhibited by a small molecule fisetin. *Oncotarget* 2014;5:2462–74.
24 Liu S, Marneth AE, Alexe G, *et al*. The kinases IKBKE and TBK1 regulate MYC-dependent survival pathways through YB-1 in AML and are targets for therapy. *Blood Adv* 2018;2:3428–42.
25 Eller C, Heydmann L, Colpitts CC, *et al*. A genome-wide gain-of-function screen identifies CDKN2C as a HBV host factor. *Nat Commun* 2020;11:2707.
26 Cui X, McAllister R, Boregowda R, *et al*. Does tyrosyl DNA Phosphodiesterase-2 play a role in hepatitis B virus genome repair? *PLoS One* 2015;10:e0128401.
27 Horwitz EM, Maloney KA, Ley TJ. A human protein containing a "cold shock" domain binds specifically to H-DNA upstream from the human gamma-globin genes. *J Biol Chem* 1994;269:14130–9.
28 Budkina KS, Zlobin NE, Kononova SV, *et al*. Cold shock domain proteins: structure and interaction with nucleic acids. *Biochemistry* 2020;85:1–19.
29 Kajino K, Yamamoto T, Hayashi J, *et al*. Recombination hot spot of hepatitis B virus genome binds to members of the HMG domain protein family and the Y box binding protein family; implication of these proteins in genomic instability. *Intervirology* 2001;44:311–6.
30 Chen C-J, Yang H-I, Su J, *et al*. Risk of hepatocellular carcinoma across a biological gradient of serum hepatitis B virus DNA level. *JAMA* 2006;295:65–73.
31 Leader M, Collins M, Patel J, *et al*. Vimentin: an evaluation of its role as a tumour marker. *Histopathology* 1987;11:63–72.
32 Lee SJ, Yoo JD, Choi SY, *et al*. The expression and secretion of vimentin in the progression of non-alcoholic steatohepatitis. *BMB Rep* 2014;47:457–62.
33 Cai D, Wang X, Yan R, *et al*. Establishment of an inducible HBV stable cell line that expresses cccDNA-dependent epitope-tagged HBeAg for screening of cccDNA modulators. *Antiviral Res* 2016;132:26–37.
34 Ise T, Nagatani G, Imamura T, *et al*. Transcription factor Y-box binding protein 1 binds preferentially to cisplatin-modified DNA and interacts with proliferating cell nuclear antigen. *Cancer Res* 1999;59:342–6.
35 Ravula AR, Teegala SB, Kalakotla S, *et al*. Fisetin, potential flavonoid with multifarious targets for treating neurological disorders: an updated review. *Eur J Pharmacol* 2021;910:174492.
36 Wang X, Lu J, Li J, *et al*. CYT387, a potent IKBKE inhibitor, suppresses human glioblastoma progression by activating the Hippo pathway. *J Transl Med* 2021;19:396.
37 Chao H-M, Huang H-X, Chang P-H, *et al*. Y-Box binding protein-1 promotes hepatocellular carcinoma-initiating cell progression and tumorigenesis via Wnt/β-catenin pathway. *Oncotarget* 2017;8:2604–16.
38 Xiao L, Zhou Z, Li W, *et al*. Chromobox homolog 8 (CBX8) interacts with Y-box binding protein 1 (YBX1) to promote cellular proliferation in hepatocellular carcinoma cells. *Aging* 2019;11:7123–49.
39 Law JH, Li Y, To K, *et al*. Molecular decoy to the Y-box binding protein-1 suppresses the growth of breast and prostate cancer cells whilst sparing normal cell viability. *PLoS One* 2010;5:e12661.

A cell-based cccDNA reporter assay combined with functional genomics identifies YBX1 as HBV cccDNA host factor and antiviral candidate target

Eloi R. Verrier[$], Gaëtan Ligat[$], Laura Heydmann, Katharina Dörnbrack, Julija Miller, Anne Maglott-Roth, Frank Jühling, Houssein El Saphira, Margaux J. Heuschkel, Naoto Fujiwara, Sen-Yung Hsieh, Yujin Hoshida, David E. Root, Emanuele Felli, Patrick Pessaux, Atish Mukherji, Laurent Mailly, Catherine Schuster, Laurent Brino, Michael Nassal[&], Thomas F. Baumert[&]

[$]co-first author. [&]co-senior authors.

ONLINE SUPPLEMENTARY MATERIAL

MATERIAL AND METHODS

Human subjects

Primary human hepatocytes (PHH) were obtained from liver tissue from patients undergoing liver resection for liver metastasis at the Strasbourg University Hospitals with informed consent. Protocols were approved by the local Ethics Committee of the Strasbourg University Hospitals (CPP) and the Ministry of Higher Education and Research of France (DC 2016 2616). PHH were isolated and cultured as described [1]. Human samples from HBV infected patients followed at the Chang Gung Memorial Hospital (Taipei, Taiwan) were obtained with informed consent. Protocols were approved by the local Ethics Committee (Institutional Review Board 102-3825C).

Patient and Public Involvement

Not applicable.

Reagents and plasmids

Dimethyl sulfoxide (DMSO), polybrene, Tween-20 and PEG 8000 (polyethylene glycol) were obtained from Sigma-Aldrich (Merck). Paraformaldehyde was obtained from Euromedex. DNA transfection was performed using CalPhos Mammalian Transfection kit (Clontech) according to the manufacturer's instructions. The shRNA-encoding lentivirus constructs were obtained from the RNAi Platform, Broad Institute of MIT and Harvard (Cambridge, USA). pTRE2-hyg plasmid was used to generate a Tet-controlled HepG2 cell line expressing a modified envelope-deficient full-length DHBV genome. Small guide (sg)RNAs were cloned into the Cas9 expressing pLKO puro plasmid (plasmid #8453, Addgene). The expression lentivirus constructs were obtained from Vectorbuilder (VB201221-1030xyb: sgRNA-resistant wild type YBX1 (YBX1-WT); VB190320-1155uyp: control vector). Vector sequences are available online (https://en.vectorbuilder.com/design/retrieve.html). Cell viability was assessed using PrestoBlue™ Cell Viability Reagent (Thermo Fisher).

Cell lines

Human embryonic kidney 293T (HEK 293T) cell line has been described [1]. Purification of infectious HBV particles from the inducible human hepatoblastoma HepAD38 has been described [2, 3]. For the production of NTCP-expressing HepG2 and Huh7 cells, cells were seeded in six-well plates at 50% confluence 1 day prior to transduction with human NTCP-expressing vesicular stomatitis virus pseudoparticles (pp) (GeneCopoeia). After 3 days, cells were expanded and selected for NTCP expression with 500 µg/mL of neomycin (G418). HepG2-NTCP and Huh7-NTCP cells were maintained at a concentration of 250 µg/mL G418.

HBV and HDV production

The production of recombinant HBV (ayw) and HDV (genotype 1) infectious virus have been described [3, 4]. The primers used for quantification of HBV RNA (both pgRNA and preC RNA) and HDV RNA by RT-qPCR following infection are indicated in Supplementary Table S3.

Establishment of a Tet-controlled HepG2 cell line expressing a modified full-length DHBV genome

DHBV-HA2/3env$^-$ (HA2/3 in brief) is a clonal cell line based on the human HepG2 hepatoma cell line derivative HepG2.TA2-7 that stably expresses the Tet-transactivator tTA2, maintained by G418 selection [5]**,** and a derivative of the TRE promoter plasmid pTRE2-hyg which carries the hygromycin resistance gene. Into this plasmid a 1.1x unit lengths DHBV16 genome (GenBank K01834) carrying a a stop mutation in the preS region (G1165A) and a HA-tag (YPYDVPDYA) coding sequence in the preC region four codons upstream (DpC_HA1) or immediately (DpC_HA2) in front of the core ORF was inserted such that TRE promoter initiates transcription at the authentic pgRNA start site. Of the resulting plasmids pTRE-DHBVpC_HA2-env$^-$ was transfected into HepG2.TA2-7 cells and stable cell clones were selected via hygromycin. Clone HA2/3 showed robust, Dox withdrawal-dependent replication initiation, cccDNA formation and HAeAg secretion. To access capsid-associated and nuclear viral DNAs, cytoplasm and nuclei were separated by NP40 lysis, then nucleocapsid-associated and nuclear DNAs were extracted and detected by Southern blotting using a ^{32}P labeled DNA probe as previously described [6], except that to the nuclei a constant amount of the 6.3 kb DHBV16 expression plasmid pCD16 was added to monitor the subsequent DNA extraction [6]. HAC18 cells were produced using the same strategy replacing DHBV by HBV genome.

Detection of DHBeAg by specific anti-HA ELISA and Immunofluorescence

HA2/3 cells were seeded in 96-well plates and doxycycline was withdrawn to allow pgRNA transcription. Supernatants were harvested at different time points for the specific detection of HA-taged DHBeAg (HA-DHBeAg) through anti-HA sandwich ELISA. 96-well microplates (Thermo Fisher Scientific) were pre-coated with anti-DHBcAg chicken Ba09 antibody at a dilution of 1:1000 overnight at 4 °C. After blocking with PBS, 10% FBS, Tween 20 (0,05%) for 3 h, the plates were washed with PBS containing 0.05% Tween 20 four times. 40 µL of each sample were incubated in the coated plates overnight at 4°C. The plates were washed with PBS containing 0.05% Tween 20 four times and incubated with mouse anti-HA-PO antibody (3F10, Roche) at a dilution of 1:1000 for 1 h. Plates were washed samples were incubated with peroxidase-conjugated, goat anti-mouse-PO IgG at a dilution of 1:5000 (NA931, GE Healthcare). After washing, the HA-DHBeAg levels were revealed with the SuperSignal™ ELISA Femto Substrate (Thermo Fisher Scientific) for 1 min. Chemiluminescence was determined at 425 nm using a Mithras LB940 Microplate reader (Berthold). For Immunofluorescence detection of DHBcAg and DHBeAg, HA2/3 cells were seeded in 96-well plates and doxycycline was withdrawn to allow pgRNA transcription. Cells were fixed with 4% paraformaldehyde (PFA). DHBcAg and HA-DHBeAg were detected using a specific mouse antibody (21-5-10c) and a specific mouse anti-HA tag antibody (HA tag antibody [HA.C5] (ab18181), respectively, and an AF647-labelled secondary antibody targeting mouse IgGs (Jackson Research). Cell nuclei were stained with DAPI. Fluorescent imaging was performed using an Axio Vert.A1 microscope (Carl Zeiss).

Targeted loss-of-function screen using a shRNA-encoding lentiviral expression library

A DNA-repair targeting shRNA library was designed and prepared at the RNAi platform from the Broad Institute of MIT and Harvard, Cambridge, USA. The 239 targeted genes are listed in Supplementary Table S1. Three shRNA constructs per gene were designed. shRNA constructs were cloned into a pLKO vector carrying the puromycin resistance gene HA2/3 cells, initially cultured in the presence of doxycycline, were plated in 96-well plates, and cultured for one day in doxycycline-free medium prior to transduction, in triplicate, with the shRNA-encoding lentiviral expression library. Cells were selected with puromycin (2 µg/ml) three days after transduction. At 21 days post platting and doxycycline withdrawal, the supernatants were

harvested for quantification of secreted HA-DHBeAg as described above. Stable and long-term shRNA-induced gene expression silencing was assessed by the quantification of YBX1 expression, one candidate of the screen, at days 10 and 21 post plating (Supplementary Figure S1). The global effect of individual gene silencing on HA-DHBeAg production was analyzed by pooling the effect of the 3-independent shRNA per gene (n=9). *p* values were obtained through a Student's t-test comparing phenotypic effects of shRNAs and pLKO ctrl. The analysis of the candidates included phenotypic robustness between replicates, toxicity (PrestoBlue™ > 0.75 compared to pLKO ctrl), and expression in the liver (Illumina Body Map).

Loss-of-function studies in HBV/HDV permissive cells and primary human hepatocytes
Individual shRNA-encoding lentiviral particles were produced in HEK 293T cells by cotransfection of plasmids expressing the human immunodeficiency virus (HIV) gag-pol, the vesicular stomatitis virus glycoprotein (VSV-G) and the pLKO.1 puro-shRNA plasmids in the ratio of 10:3:10, using the CalPhos Mammalian Transfection kit as described [1]. Three days after transfection, supernatants were collected and clarified using 0.45 µm pore filters. HepG2-NTCP were transduced with shRNA-encoding lentivirus and selected with puromycin 2 µg/mL 48 hours prior to HBV infection. Alternatively, PHH were transduced with individual shRNA-containing lentivirus prior to HBV infection. To generate YBX1-KO HepG2-NTCP and Huh7-NTCP cell lines, the following primers corresponding to guide RNAs targeting YBX1 exons were cloned into the generated Cas9 expressing pLKO puro plasmid (plasmid #8453, Addgene): Forward primer: CACCGACGGATATGGTTTCATCAAC, Reverse primer: AAACGTTGATGAAACCATATCCGTC. For robust KO early stage passages of cells need to be used. For rescue experiments, YBX1-KO HepG2-NTCP were transduced with ctrl vector, or YBX1-WT-containing lentivirus constructs and selected with puromycin 48 hours prior to HBV infection. HepG2-NTCP and PHH were infected by HBV (GEq 500 per cell and 1500 per cell, respectively) as described [7]. HBV infection was assessed 10 days post infection (dpi) by quantification of HBeAg using chemiluminescence immunoassay (CLIA, Autobio) following the manufacturer's instructions. Alternatively, cells were lysed and total RNA was extracted using the ReliaPrep RNA Miniprep Systems (Promega) and qRT-PCR quantification of HBV pgRNA was performed as described [3]. Alternatively, cells were fixed with 4% PFA. HBsAg was immunodetected using a specific mouse monoclonal anti-HBsAg antibody (clone 1044/329, Bio-Techne, USA) and Alexa Fluor 647-labelled secondary antibody targeting mouse IgGs (Jackson Research). Cell nuclei were stained with DAPI. Fluorescent imaging was performed using an Axio Vert.A1 microscope (Carl Zeiss). In addition, YBX1-KO Huh7-NTCP cells were produced as described above for YBX1-KO HepG2-NTCP cells and infected with HDV. HDV infection was assessed 7 dpi by qRT-PCR quantification of HDV RNA or immunodetection of HDAg as described [4]. Fluorescent imaging was performed using an Axio Vert.A1 microscope (Carl Zeiss).

cccDNA detection by Southern blot and qPCR.
Southern blot detection of HBV cccDNA was performed using digoxigenin (DIG)-labeled (Roche) specific probes as described [8]. Total DNA from HBV-infected cells was extracted using the Hirt method as described [9]. Specific DIG-labeled probes for the detection of HBV and mitochondrial DNAs were synthetized using the PCR DIG Probe Synthesis Kit (Roche) and the primers as described [7]. DNA Molecular Weight Marker II and VII (Roche) were used. cccDNA levels were quantified using ImageJ software.
Specific cccDNA qPCR method was already described [8, 10]. DNA was extracted with a protocol adapted from the MasterPureTM DNA Purification Kit (Epicentre).
The following primers and probes were used:
cccDNA Taqman Probe 1864-1882: [6FAM]CATGGAGACCACCGTGAACGCCC[BHQ1] (final concentration: 0.2µM) ;
FW Primer: CCGTGTGCACTTCGCTTCA (final concentration: 0.1µM)
RV Primer: GCACAGCTTGGAGGCTTGA (final concentration: 0.8µM).
cccDNA levels were normalized to βglobin levels (TaqMan® Gene Expression Assay, Hs00758889_s1, Life Technologies).

Analysis of gene expression by RT-qPCR
RNA was extracted as described above and gene expression was assessed by qRT-PCR as described [7]. Gene expression was normalized to GADPH expression. Primers and TaqMan® probes for POLK (Hs00211965_m1), TDP2 (Hs01099017_m1), YBX1 (Hs00358903_g1) and PCNA (Hs00427214_g1) mRNA quantification were obtained from ThermoFisher (TaqMan® Gene Expression Assays, Life Technologies).

Analysis of protein expression by Western blot
The protein expression of YBX1, phospho-YBX1 (S102), GAPDH and β-actin was assessed by Western blot as described [7] using a monoclonal rabbit anti-YBX1 antibody (ab76149, Abcam), a polyclonal rabbit anti-YBX1(phospho S102) antibody (ab138654, Abcam) a polyclonal rabbit anti-GAPDH (ab9485, Abcam), and a monoclonal mouse anti-β-actin (A5441, Sigma), respectively. Protein expression was assessed using the ChemiDocTM Imaging System (Bio-Rad).

Prediction of a putative Y-box motif within HBV genome
The HBV genome sequence of reference strain ayw and adw was aligned with the Y-box consensus sequence. Alignments were performed with Clustal Omega (Ω) multiple sequence alignment (MSA) tool provided by the EMBL-EBI bioinformatics web and programmatic tools framework [11].

ChIP-qPCR Assay
HepG2-NTCP were infected by HBV (GEq 500 per cell) as described [7]. The ChIP protocol was adapted from [12] with few minor modifications. Two days post infection, fresh formaldehyde was added [0.4% final concentration (v/v)] to the PBS containing cells and incubated on a flip-flop rocker for 10 min at room temperature, followed by addition of 2M glycine (0.125M final concentration) quenched with 0.25 M glycine for 5 min, and mechanically lysed at 4°C in lysis buffer (PIPES 5 mM, KCL 85 mM, NP-40 0.5%), with protease inhibitors (Roche). After low-speed centrifugation, nuclei were lysed in SDS-buffer (EDTA 10 mM, Tris-HCl pH8 50 mM, SDS 1%). After sonication (Covaris), clarified lysates were diluted in RIPA-buffer (Tris-HCl pH-7.5 10 mM, NaCl 140 mM, EDTA 1 mM, EGTA 0.5 mM, 1% Triton-X100, 0.1% SDS, 0.1% Na-Deoxycholate). Nuclear lysates were precleared with magnetic protein G-beads (10004D, Invitrogen) before immunoprecipitation with rabbit IgG isotype control (ChIP grade, ab76149, Abcam), a rabbit anti-YBX1 antibody (ab76149, Abcam) or an anti-HBcAg antibody (MA1-7607, Invitrogen) at 4°C. Magnetic beads were added for 2 h to capture immune complexes. Flow-through fractions were collected, and beads washed with RIPA-buffer. Immunoprecipitated complexes were either boiled in Laemmli 1X for western blot analysis or washed with TE (Tris-HCl pH-8 10 mM, EDTA 10 mM) and then incubated for 2 h at 68°C in elution buffer (Tris-HCl pH-7.5 20 mM; EDTA 5 mM; NaCl 50 mM; 1% SDS; Proteinase-K 50 µg/ml). DNA was then extracted and quantified by qPCR using specific primers (TaqMan® Gene Expression Assay, HBV, ID Pa03453406, Life Technologies) as described [12, 13]. DNA was similarly purified from the flow-through fraction and used as input for calculations. Protein expression in each sample was assessed by Western blot using a a rabbit anti-YBX1 antibody (ab76149, Abcam) or an anti-HBcAg antibody (MA1-7607, Invitrogen), and VeriBlot for IP Detection Reagent (HRP) (ab131366, Abcam).

Infection of FRG-NOD mice for ChIP-qPCR assay.
We used HBV-infected FRG-NOD mice from the cohort of a previously published study [14]. Mice were housed and bred at the INSERM U1110 animal facility (regional agreement n°E-67-482-7) and fed 2-(2-nitro-4-trifluoromethylbenzoyl)-1,3-cyclohexanedione (NTBC) in their drinking water (16 mg/L). Six-week-old FRG-NOD mice received 1.5×10^9 pfu of an adenoviral vector encoding for the urokinase-like plasminogen activator, and treated with NTBC (8 mg/L). Forty eight hours later mice were intrasplenically transplanted with 10^6 PHHs (Corning) and given NTBC at 0.8 mg/L. During the following days NTBC dose was decreased every 2 days to 0.4 mg/L and 0.2 mg/L, and finally withdrawn. Efficient transplantation was assessed 8

weeks later by measuring human serum albumin levels by ELISA (Bethyl). The transplantation procedure was approved by the local Ethics committee and authorized by the French ministry of research and higher education (APAFIS#4485-2016031115352125 v3). Successfully transplanted mice were infected with 10^9 HBV (ayw) genome equivalents. The experimental procedure was approved by the local Ethics committee and authorized by the French ministry of research and higher education (APAFIS#13872-2018050214497349 v1). Human albumin levels were determined as described previously [15]. Mice were sacrificed and livers harvested after 10 weeks of HBV infection. 3 "control" mice from the [14] study were used. HBV DNA viral load was determined at the time of sacrifice using the clinically approved Abbott Real Time HBV assay (Abbott). Human albumin levels were determined as described previously [15]. Viral loads and albumin levels per mouse are presented in Supplementary Table S4. Liver samples were lyzed and ChIP-qPCR assay for HBV DNA quantification upon immunoprecipitation using a specific anti-YBX1 antibody was performed as described above. The only difference is the use a Bioruptor (Diagenode) device for the sonication of samples.

Analysis of YBX1 expression in patients.

For the analysis of YBX1 mRNA expression in patients, total RNA was extracted from liver tissue of 9 HBV-infected patients by using High Pure RNA Paraffin kit (Roche) according to the manufacturer's instruction, and gene expression analysis was performed by RNA-seq as previously reported [16]. To analyze the correlation between YBX1 expression and the progression of liver disease in HBV-infected patients, YBX1 mRNA expression was assessed in HBV-related patients from GSE121248 [17]. For survival and recurrence analysis, data of HBV-induced HCC patients were derived from GSE14322 [18]. To analyze the correlation between YBX1 expression and the NASH fibrosis stage, YBX1 mRNA expression was assessed in HBV-related patients from GSE49541 [19]. For survival and HCC development analysis, data of HCV-induced HCC patients were derived from GSE14322 [20].

Statistical analyses

Statistical analyses were performed using a two-tailed Mann-Whitney U test unless otherwise stated; $p < 0.05$ (★), $p < 0.01$ (★★), and $p < 0.001$ (★★★) were considered statistically significant. Correlation between YBX1 expression and HBV viral load in patients was assessed using Spearman's rank correlation coefficient (Spearman's rho). Survival functions depending on YBX1 expression were obtained using the Kaplan-Meier estimator. *p*-value was calculated using log-rank test for comparisons of Kaplan-Meier survival. $p < 0.05$ was considered statistically significant. Significant *p*-values are indicated by asterisks in the individual figures and figure legends.

SUPPLEMENTARY FIGURES

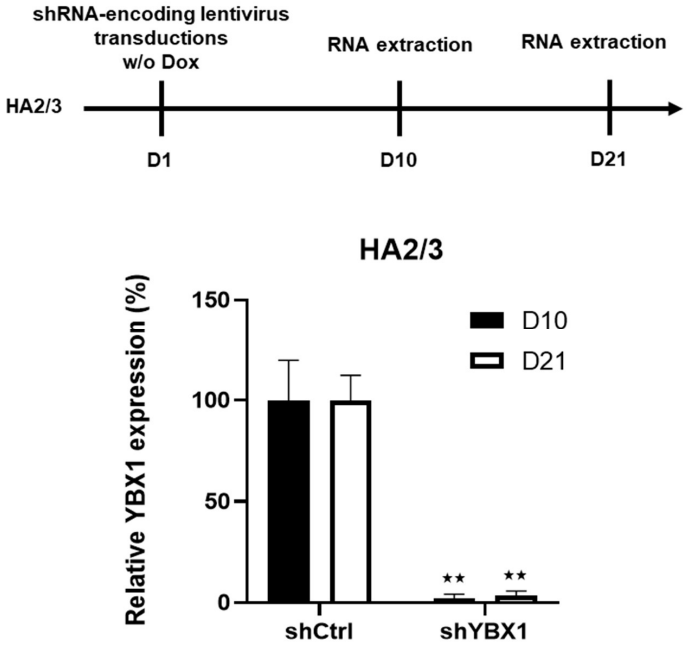

Figure S1: Control of long-term silencing of YBX1 expression in HA2/3 cells. HA2/3 cells were plated in 96well-plates one day prior to transduction. YBX1 expression was assessed by qRT-PCR at day 10 and day 21 post platting. Results are expressed as means ± SD % relative YBX1 expression compared to shCtrl (set at 100%) from 3 independent experiments. ★★ p < 0,01 (two-tailed Mann–Whitney U test).

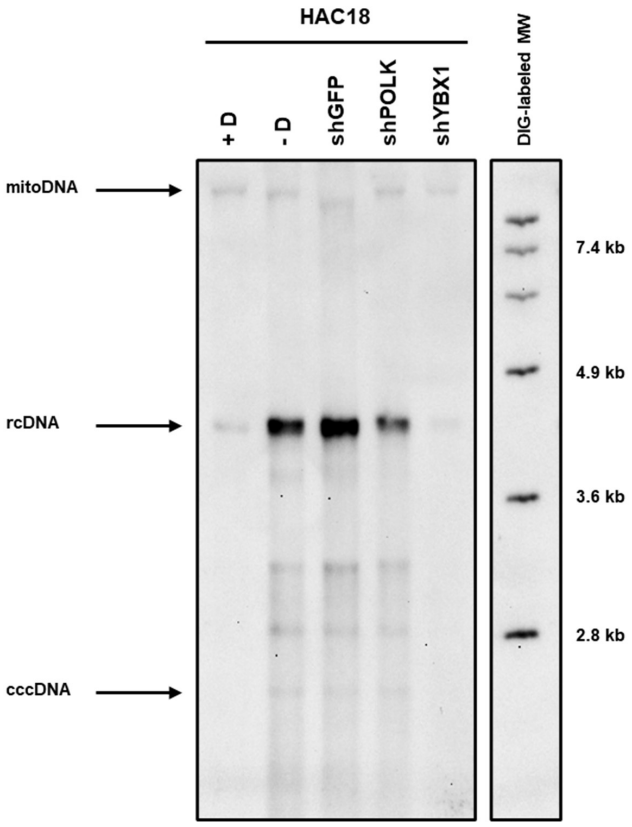

Figure S2: POLK- and YBX1 specific knock-down decreases cccDNA levels in HAC18 cells. HAC18 were transduced with shRNA-encoding lentivirus, without Dox and selected with puromycin 2 µg/mL 48 hours. Detection of HBV DNAs by Southern Blot 21 days post platting. HBV rcDNA and HBV cccDNA are indicated.

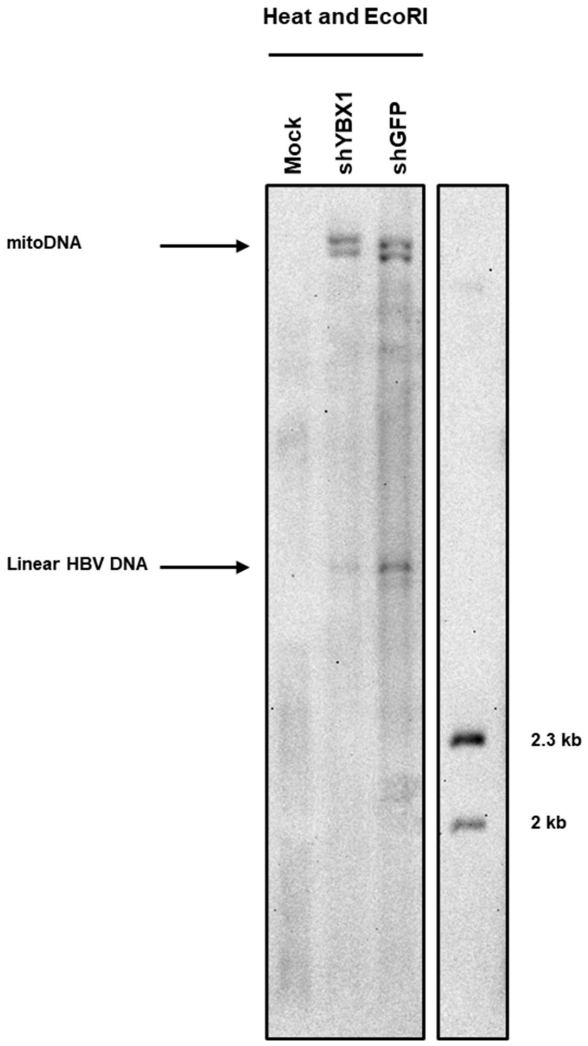

Figure S3: Linearization of HBV cccDNA. HBV DNAs were submitted to heat treatment (85°C) and subsequent EcoRI digestion (control related to the Figure 4J).

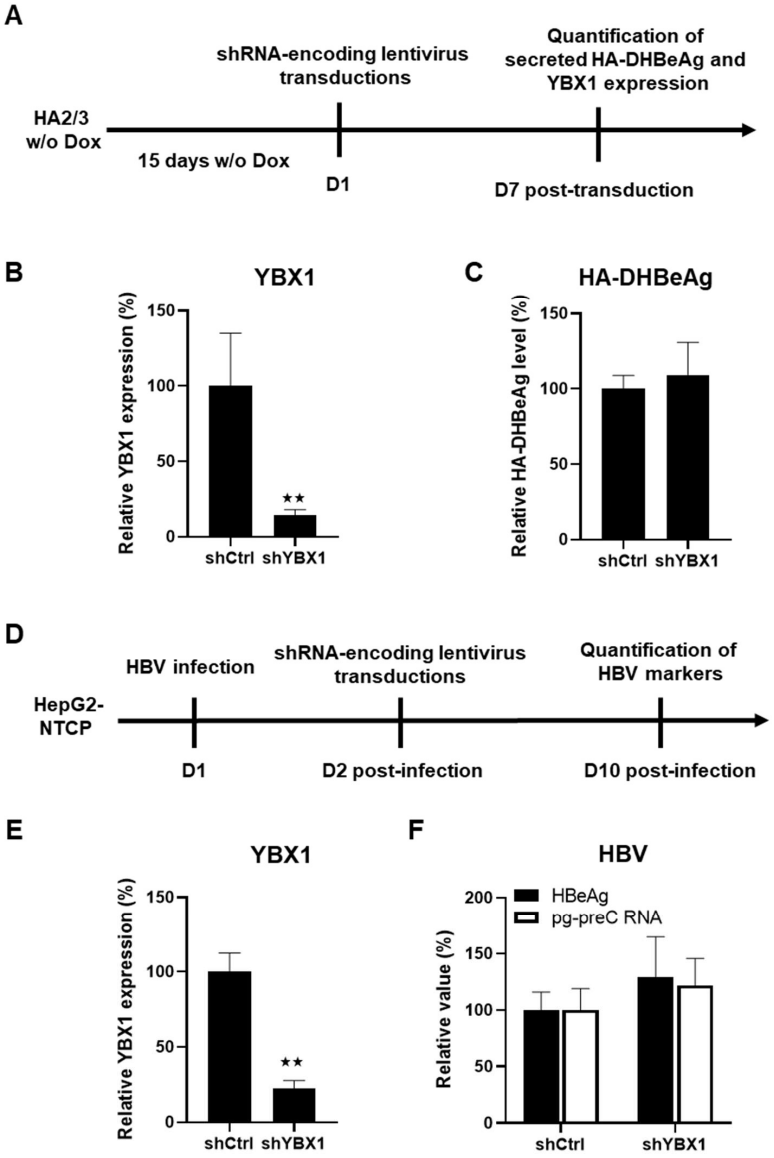

Figure S4: YBX1 knock-down after establishment of the cccDNA pool affects HBV replication neither in HA2/3 cells nor in infected HepG2-NTCP cells. A. Experimental timelines. **B.** YBX1 mRNA expression upon silencing, assessed by qRT-PCR. Results are expressed as means ± SD % relative YBX1 expression compared to shCtrl (set at 100%) from three independent experiments. **C.** HA-DHBeAg production quantified by anti-HA ELISA 7 days after transduction. Results are expressed as means ± SD % relative HA-HBeAg secretion compared to shCtrl (set at 100%) from three independent experiments. **D.** Experimental timelines. **E.** YBX1 mRNA expression upon silencing; assessed by qRT-PCR. Results are expressed as means ± SD % relative YBX1 expression compared to shCtrl (set at 100%) from three independent experiments. **F.** Detection of HBV markers 10 dpi: HBeAg is quantified by CLIA (black), HBV pg-preC RNA is quantified by qRT-PCR (white). Results are expressed as means ± SD % relative HBV infection compared to shCtrl (set as 100%) from 3 independent experiments. ★★ $p < 0,01$ (two-tailed Mann–Whitney U test).

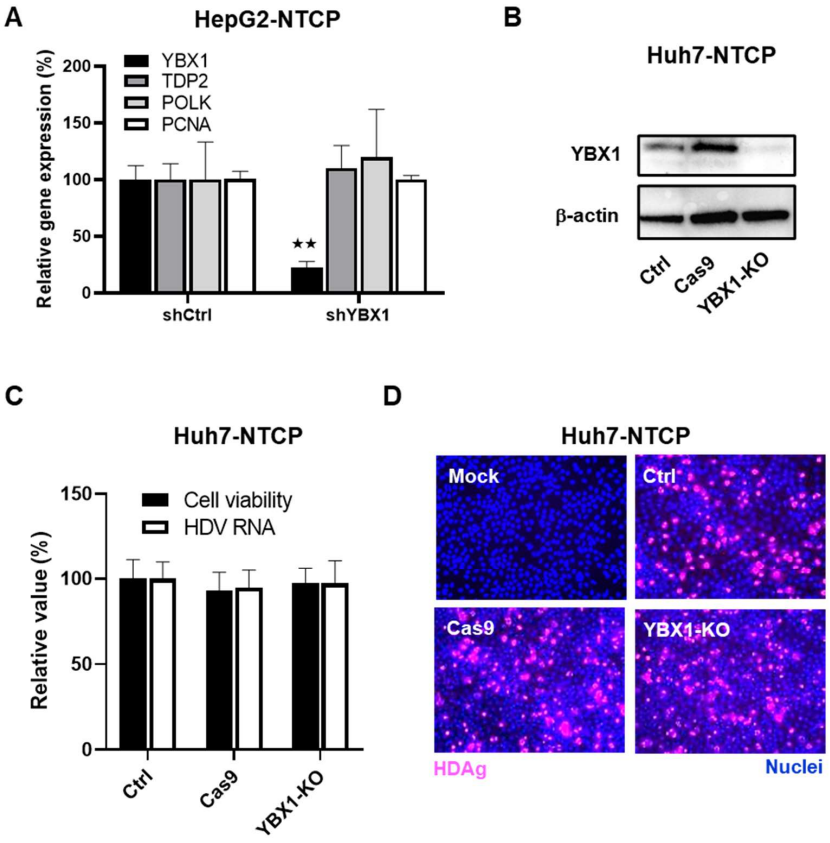

Figure S5. Impact of YBX1 expression on the early steps of the HBV life cycle. A. YBX1 silencing does not modulate the expression of cccDNA-related factors. YBX1 expression was silenced in HepG2-NTCP cells using specific shRNA. Silencing efficacy was assessed by YBX1 mRNA quantification by qRT-PCR. Samples from Figure S4E were used. The expression of YBX1, POLK, TDP2, and PCNA was analyzed by qRT-PCR. Results are expressed as means ± SD % relative expression compared to shCtrl (set at 100%) from 3 independent experiments. **B-D.** No effect of YBX1 KO on HDV infection in Huh7-NTCP cells. YBX1 expression was controlled by Western blot in Huh7-NTCP (ctrl), cas9-expressing Huh7-NTCP cells (cas9), and YBX1-KO Huh7-NTCP (**B**). Cells were then infected by HDV for 7 days. Cell viability was assessed 7 dpi. Results are expressed as means ± SD % relative cell viability compared to HDV-infected Huh7-NTCP (set at 100%) from 2 independent experiments (black) In parallel, total RNA was extracted and HDV infection was assessed by quantification of HDV RNA by RT-qPCR (white) (**C**). Results are expressed as means ± SD % relative HDV infection compared to HDV-infected Huh7-NTCP (set as 100%) from 2 independent experiments. Alternatively, intracellular HDAg levels were assessed by IF 7 dpi (**D**). ★★ $p < 0,01$ (two-tailed Mann–Whitney U test).

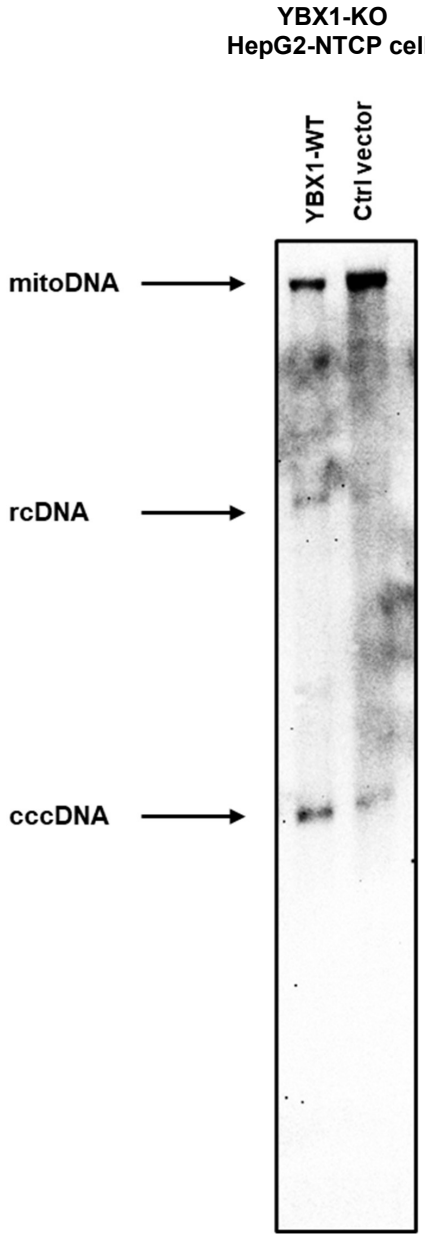

Figure S6: Expression of YBX1 increases cccDNA levels in YBX1-KO cells. YBX1-KO HepG2-NTCP cells were transduced with lentivirus encoding the wild type version of YBX1 (YBX1-WT) or an empty vector (control). 6 days after transduction, cells were infected by HBV. 2 days post infection, DNA was extracted and HBV DNA was detected by Southern blot.

SUPPLEMENTARY REFERENCES

1. Lupberger J, Zeisel MB, Xiao F, et al. EGFR and EphA2 are host factors for hepatitis C virus entry and possible targets for antiviral therapy. *Nat Med*. 2011;17(5):589-95.

2. Ladner SK, Otto MJ, Barker CS, et al. Inducible expression of human hepatitis B virus (HBV) in stably transfected hepatoblastoma cells: a novel system for screening potential inhibitors of HBV replication. *Antimicrob Agents Chemother*. 1997;41(8):1715-20.

3. Verrier ER, Colpitts CC, Bach C, et al. A targeted functional RNA interference screen uncovers glypican 5 as an entry factor for hepatitis B and D viruses. *Hepatology*. 2016;63(1):35-48.

4. Verrier ER, Weiss A, Bach C, et al. Combined small molecule and loss-of-function screen uncovers estrogen receptor alpha and CAD as host factors for HDV infection and antiviral targets. *Gut*. 2020;69(1):158-67.

5. Schreiner S, Nassal M. A Role for the Host DNA Damage Response in Hepatitis B Virus cccDNA Formation-and Beyond? *Viruses*. 2017;9(5).

6. Kock J, Rosler C, Zhang JJ, et al. Generation of covalently closed circular DNA of hepatitis B viruses via intracellular recycling is regulated in a virus specific manner. *PLoS Pathog*. 2010;6(9):e1001082.

7. Verrier ER, Yim SA, Heydmann L, et al. Hepatitis B Virus Evasion From Cyclic Guanosine Monophosphate-Adenosine Monophosphate Synthase Sensing in Human Hepatocytes. *Hepatology*. 2018;68(5):1695-709.

8. Lucifora J, Salvetti A, Marniquet X, et al. Detection of the hepatitis B virus (HBV) covalently-closed-circular DNA (cccDNA) in mice transduced with a recombinant AAV-HBV vector. *Antiviral Res*. 2017;145:14-9.

9. Gao W, Hu J. Formation of hepatitis B virus covalently closed circular DNA: removal of genome-linked protein. *J Virol*. 2007;81(12):6164-74.

10. Allweiss L, Volz T, Giersch K, et al. Proliferation of primary human hepatocytes and prevention of hepatitis B virus reinfection efficiently deplete nuclear cccDNA in vivo. *Gut*. 2018;67(3):542-52.

11. Sievers F, Wilm A, Dineen D, et al. Fast, scalable generation of high-quality protein multiple sequence alignments using Clustal Omega. *Mol Syst Biol*. 2011;7:539.

12. Lucifora J, Pastor F, Charles E, et al. Evidence for long-term association of virion-delivered HBV core protein with cccDNA independently of viral protein production. *JHEP Rep*. 2021;3(5):100330.

13. Lucifora J, Bonnin M, Aillot L, et al. Direct antiviral properties of TLR ligands against HBV replication in immune-competent hepatocytes. *Sci Rep*. 2018;8(1):5390.

14. Zhuang X, Forde D, Tsukuda S, et al. Circadian control of hepatitis B virus replication. *Nat Commun*. 2021;12(1):1658.

15. Mailly L, Xiao F, Lupberger J, et al. Clearance of persistent hepatitis C virus infection in humanized mice using a claudin-1-targeting monoclonal antibody. *Nat Biotechnol*. 2015;33(5):549-54.

16. Nakagawa S, Wei L, Song WM, et al. Molecular Liver Cancer Prevention in Cirrhosis by Organ Transcriptome Analysis and Lysophosphatidic Acid Pathway Inhibition. *Cancer Cell*. 2016;30(6):879-90.

17. Wang SM, Ooi LL, Hui KM. Identification and validation of a novel gene signature associated with the recurrence of human hepatocellular carcinoma. *Clin Cancer Res*. 2007;13(21):6275-83.

18. Roessler S, Long EL, Budhu A, et al. Integrative genomic identification of genes on 8p associated with hepatocellular carcinoma progression and patient survival. *Gastroenterology*. 2012;142(4):957-66 e12.

19. Murphy SK, Yang H, Moylan CA, et al. Relationship between methylome and transcriptome in patients with nonalcoholic fatty liver disease. *Gastroenterology*. 2013;145(5):1076-87.

20. Hoshida Y, Villanueva A, Sangiovanni A, et al. Prognostic gene expression signature for patients with hepatitis C-related early-stage cirrhosis. *Gastroenterology*. 2013;144(5):1024-30.